HHS Public Access

Author manuscript

Free Radic Biol Med. Author manuscript; available in PMC 2017 August 01.

Published in final edited form as:

Free Radic Biol Med. 2016 August ; 97: 292–306. doi:10.1016/j.freeradbiomed.2016.06.025.

Alpha-synuclein modulates retinal iron homeostasis by facilitating the uptake of transferrin-bound iron: Implications for visual manifestations of Parkinson's disease

Shounak Baksi, **Ajai K Tripathi**, and **Neena Singh***

Department of Pathology, School of Medicine, Case Western Reserve University, Cleveland, Ohio 44106, USA

Abstract

Aggregation of α-synuclein (α-syn) in neurons of the substantia nigra is diagnostic of Parkinson's disease (PD), a neuro-motor disorder with prominent visual symptoms. Here, we demonstrate that α-syn, the principal protein involved in the pathogenesis of PD, is expressed widely in the neuroretina, and facilitates the uptake of transferrin-bound iron (Tf-Fe) by retinal pigment epithelial (RPE) cells that form the outer blood-retinal barrier. Absence of α-syn in knock-out mice (α-syn$^{-/-}$) resulted in down-regulation of ferritin in the neuroretina, indicating depletion of cellular iron stores. A similar phenotype of iron deficiency was observed in the spleen, femur, and brain tissue of α-syn$^{-/-}$ mice, organs that utilize mainly Tf-Fe for their metabolic needs. The liver and kidney, organs that take up significant amounts of non-Tf-bound iron (NTBI), showed minimal change. Evaluation of the underlying mechanism in the human RPE47 cell line suggested a prominent role of α-syn in the uptake of Tf-Fe by modulating the endocytosis and recycling of transferrin (Tf)/transferrin-receptor (TfR) complex. Down-regulation of α-syn in RPE cells by RNAi resulted in the accumulation of Tf/TfR complex in common recycling endosomes (CREs), indicating disruption of recycling to the plasma membrane. Over-expression of exogenous α-syn in RPE cells, on the other hand, up-regulated ferritin and TfR expression. Interestingly, exposure to exogenous iron increased membrane association and co-localization of α-syn with TfR, supporting its role in iron uptake by the Tf/TfR complex. Together with our observations indicating basolateral expression of α-syn and TfR on RPE cells *in vivo*, this study reveals a novel function of α-syn in the uptake of Tf-Fe by the neuroretina. It is likely that retinal iron dyshomeostasis due to impaired or altered function of α-syn contributes to the visual symptoms associated with PD.

Graphical abstract

*Corresponding author: neena.singh@case.ed.

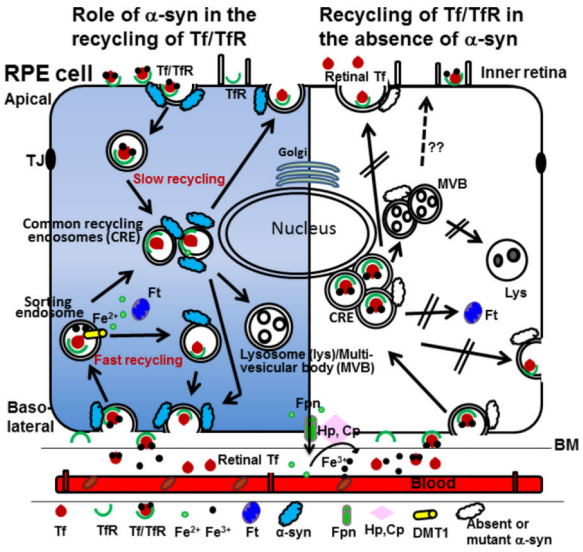

Keywords

α synuclein; retina; retinal pigment epithelial cells; transferrin-bound iron; transferrin receptor; Parkinson's disease

Introduction

Parkinson's disease (PD) is a neuro-motor disorder resulting from the progressive loss of dopaminergic (DA) neurons in the substantia nigra pars compacta (SN). Surviving neurons accumulate Lewy bodies, cytoplasmic inclusions comprised mainly of α-synuclein (α-syn) [1, 2]. The majority of PD cases are sporadic, though a small percentage is linked to mutations in genes designated *PARK 1–18* [3]. *PARK1* encodes for α-syn, a ubiquitously expressed protein responsible for most cases of sporadic PD and certain genetic forms linked to mutations in the α-syn gene [4]. Over-expression of α-syn due to gene duplication is sufficient to induce early onset autosomal dominant form of PD, supporting its central role in PD pathogenesis [5]. Although the underlying mechanism is not clear, α-syn is partly responsible for the loss of dopaminergic neurons in the SN, resulting in the motor and non-motor symptoms of PD [2, 6]. Among the non-motor symptoms, impairment of visual acuity, contrast sensitivity, color vision, and motion perception are believed to result from changes in retinal morphology and physiology [7, 8], prompting the use of non-invasive techniques such as optical coherence tomography (OCT) and visual-evoked potentials as diagnostic and prognostic tests for PD. [9–13]. The accuracy of these methods, however, is debatable [14, 15]. A better understanding of the physiological role of α-syn in the neuroretina is necessary to improve the clinical accuracy of these procedures.

One of the causes of PD-associated visual symptoms is reduced levels of dopamine in the neuroretina [16–18]. Since α-syn is expressed widely in the vertebrate retina including humans [19], it is likely that loss or dysfunction of α-syn at this site is responsible for this change. Two possible pathways of α-syn-mediated reduction of dopamine in the SN of PD cases have been proposed: 1) loss or alteration of physiological activity of α-syn, and 2)

gain of toxic function by its aggregated form [20]. A complete understanding of either pathway is lacking. It is likely that both processes contribute to varying degrees as the disease progresses. Possibilities in the former category include loss or impaired activity of α-syn in chaperoning the SNARE (soluble N-ethylmaleimide-sensitive factor attachment protein receptor) complex assembly required for the fusion of exocytic vesicles with the plasma membrane [21–24], interaction with clathrin and recycling of clathrin-coated vesicles [25, 26], synthesis, release, and re-uptake of dopamine [4, 27], and impairment of the autophagy pathway [28]. However, deletion of α-syn in transgenic mice (α-syn$^{-/-}$) fails to produce an overt phenotype except for minor abnormalities in dopamine metabolism and late stages of hematopoiesis and lymphopoiesis [29, 30], leading to the belief that toxic gain of function by aggregated α-syn is the principal cause of PD-associated pathology and symptomatology. This concept is further supported by genetic forms of PD where over-expression or aggregation of α-syn is sufficient to induce PD [5]. Though plausible in the SN, this is an unlikely cause of ocular pathology because aggregation of α-syn is relatively rare in the neuroretina [9, 31, 32]. Loss of α-syn function, therefore, is a more likely cause of dopamine deficiency in the neuroretina and associated visual symptoms.

How might α-syn influence dopamine metabolism in the neuroretina? The principal cells that synthesize dopamine in the neuroretina are amacrine cells, inter-plexiform cells, and RPE cells [18]. The latter are of particular interest because transplanted RPE cells in the SN produce sufficient amounts of dopamine to replace degenerated dopaminergic neurons, a procedure under trial as a viable therapeutic option for PD [33–35]. Likewise, supplementation with L-DOPA, a precursor of dopamine, improves the clinical outcome of age-related macular degeneration (AMD), a condition associated with dysfunction of RPE cells and apparently unrelated to PD [36]. Although α-syn has not been implicated in the pathogenesis of AMD *per se*, it is expressed in RPE cells, where it is likely to modulate dopamine synthesis and/or metabolism [28, 29, 37].

Another feature shared by PD and AMD is accumulation of iron in the affected regions; SN in PD, and RPE cells in AMD [38–41]. This observation is of particular interest because α-syn influences cellular iron levels, and is itself regulated by iron. In support of the former, the C-terminus of α-syn has specific binding sites for iron [42, 43], a property that is likely to influence cellular iron levels. Secondly, α-syn is believed to function as a ferrireductase, facilitating the transport of ferric iron across membranes through metal transporters [44]. In support of the latter, iron is believed to modulate the synthesis of α-syn at the translational level through a putative iron responsive element in the 5'-UTR of its mRNA [45, 46]. Excess iron, on the other hand, aggregates α-syn [47] and converts dopamine to a toxic oxidation product [48, 49], resulting in the loss of functional activity of both α-syn and dopamine. Interestingly, α-syn is known to interact with clathrin and modulate the trafficking of transferrin/ transferrin receptor (Tf/TfR) complex, raising the possibility that it could mediate the uptake Tf-iron (Tf-Fe) through this pathway [25, 50]. Dysfunction of α-syn is therefore likely to alter cellular iron homeostasis, and secondarily, dopamine metabolism. It is interesting to note that iron deficiency is associated with reduced expression of dopamine receptors and dopamine transporter on synaptic membranes, reducing the overall content of dopamine [51, 52], and iron dyshomeostasis is believed to cause degeneration of dopaminergic neurons [53]. An important example is restless-leg-syndrome (RLS), a

disorder associated with brain iron deficiency with a secondary defect in the uptake and utilization of dopamine [52, 54]. L-DOPA is an effective therapeutic option for RLS, supporting the intimate relationship between iron and dopamine metabolism. Iron is also essential for the conversion of all-trans-retinyl ester to 11-cis-retinol in the visual cycle, where it is necessary for the isomerohydrolase activity of RPE65 [55]. Thus, dysfunction of α-syn is likely to set in motion a series of events culminating in the dysregulation of cellular iron and dopamine metabolism, with iron as the critical component that influences the expression and function of α-syn, and is itself modulated by α-syn (Schematic 1).

Here, we investigated the role of α-syn in iron uptake by RPE cells, the site of dopamine synthesis and an integral component of the outer blood-retinal barrier that separates the neuroretina from fenestrated choroidal capillaries [50, 56, 57]. The polarized nature of these cells confers distinct structural and functional properties to each domain necessary for their specialized function. The AP membrane interdigitates with the light-sensitive photoreceptor outer segments and regenerates visual pigments by phagocytosing and degrading shed tips of outer segments [58]. This process releases significant amounts of iron which, unless exported, binds RPE cell melanin and can reach toxic concentrations. The BL membrane is separated from choroidal capillaries by the Bruch's membrane, and regulates the transport of iron and other nutrients through specific transporters and receptors [50, 59]. Uptake of iron is mediated by the well-known Tf/TfR pathway, and export is accomplished by the iron export protein ferroportin (Fpn) coupled with the ferroxidase activity of ceruloplasmin (Cp) and hephaestin (Hp). Clear evidence for the expression of divalent metal transporters on the plasma membrane of RPE cells is lacking, though transcripts of several members of the ZIP family of proteins have been detected in RPE19 cells [60]. Thus, Tf-Fe is likely the main source of iron for the neuroretina and other ocular tissues [61].

We report that α-syn modulates the trafficking of Tf/TfR complex, thereby facilitating the uptake of Tf-Fe by the neuroretina and other visceral organs. Absence or down-regulation of α-syn disrupts this pathway, resulting in iron deficiency in the retina and other organs where Tf-Fe is the principal source of iron for metabolic purposes. These observations reveal a novel function of α-syn in retinal iron homeostasis, and provide insight into the mechanism underlying PD-associated retinal pathology and visual symptoms.

Materials and Methods

Animals and ethics statement

α-Syn knockout mice (cat # 003692) mice were procured from the Jackson laboratory and bred with wild-type mice with the C57BL/6NJ background. Animals from the F2 generation were used to generate homogenous wild type (α-syn$^{+/+}$) and knockout (α-syn−/−) mice. Up to three generations were used for experiments. Animals were housed in AAALAC-accredited facilities of the CWRU School of Medicine (SOM) under a 12-h day-night cycle and had *ad libitum* access to food and water. Standard Operating Procedures for animal use available from the IACUC office were followed. The animal health program was directed by Dr. Durfee, DVM, Diplomate ACLAM, and provided by two full-time veterinarians. Animals were observed daily for signs of illness by the animal technician responsible for providing husbandry. Medical records and documentation of experimental use were

maintained by cage group. The experiments listed in this study were approved as per protocol # 2015–0027 by the CWRU IACUC committee.

Antibodies and Chemicals

The following primary antibodies were used for this study: ferritin-H (sc-25617) and β-globin (sc-21757) from Santa Cruz Biotechnology Inc, USA, TfR from Invitrogen, USA (13–6800), α-syn from BD transduction, USA (#610786), ZIP8 (SAB3500598), ZIP14 (HPA016508), and ferritin (F5012) from Sigma, USA, β-actin (MAB1501) and RPE65 (MAB5428) from Millipore, USA, and LAMP1 (ab24170) and α-globin (ab102758) from Abcam, USA. HRP-conjugated secondary antibodies were purchased from GE healthcare, (NA 931V, NA 934V) UK, FITC (4010-02, 1010-02) and Alexa fluor 546 (A11071, A11018) tagged secondary antibodies were from Southern Biotech, USA and Molecular Probes, Invitrogen, USA respectively, and rhodamine tagged transferrin (T-2872) was from Thermo scientific, USA. Ferric ammonium citrate (FAC) (F5879), ferrous ascorbate (A0207) and desferrioxamine (D9533) and all other general chemicals were purchased from Sigma Aldrich, USA.

Cell lines and culture conditions

The immortalized human retinal pigment epithelial cell line RPE47 was a kind gift of Dr. Feng Lin, Cleveland Clinic Foundation, OH,USA [62]. Cells were cultured in DMEM supplemented with 10% heat inactivated FBS at 37°C and 5% CO_2 in a humidified atmosphere, and passaged every third day. Transfection was performed using lipofectamine 3000 (Invitrogen) according to manufacturer's protocol.

Plasmid constructs

The plasmid construct encoding human α-syn was purchased from origene, USA (SC119919), and sub-cloned into piggybac (#748) and piggybac EGFP (#740) vectors (Systems Biosciences, CA, USA) using 5'-GTCGACATGGATGTATTCATGAAAGGA CTTTC −3' forward and 5'-TCTAGATTAGGCTTCAGGTTCGTAGTCTTG −3' reverse primers. All constructs were sequenced before transfection. Transfected cells were selected in the presence of blasticidin S and stable cells were used for all experiments. Plasmid encoding α-syn A53T–EGFP was purchased from Addgene (#40823).

RNAi knockdown

siRNA against α-syn (sc-29619) and control siRNA (sc-37007) were purchased from Santa Cruz Biotechnology Inc, USA. RPE47 cells were transfected with siRNA using Lipofectamine RNAi max from Invitrogen, and knock-down of α-syn was confirmed by Western blotting.

SDS-PAGE, Western blotting, and native gel electrophoresis

Samples prepared in RIPA lysis buffer (50mM Tris-Cl pH7.4, 100mM NaCl, 1% NP-40, 0.5% deoxycholate) were clarified by centrifugation, boiled in reducing gel-loading buffer, and fractionated by SDS-PAGE. Proteins transferred to PVDF membrane were probed with specific antibodies. For fractionating ^{59}Fe-labeled proteins, samples were homogenized in

native lysis buffer (0.14M Nacl, 1.5% Triton-X-100, 0.1 M HEPES, 1mM PMSF), fractionated by native PAGE, and visualized by autoradiography. Quantification of protein bands was performed by densitometry using UN-SCAN-IT gels (version6.1) software (Silk Scientific) and represented graphically using GraphPad Prism (Version 5.0) software (GraphPad Software Inc.). Dilutions of antibodies used for immunoblotting were Ferritin (1:1000), α-syn (1:2000), β-actin (1:10,000), RPE65 (1:1000), TfR (1:2000), α-globin (1:1000), β-globin (1:1000), HRP-mouse (1:15,000), HRP-rabbit (1:15,000).

Immunostaining

Enucleated eyes were fixed in 4% paraformaldehyde in PBS overnight followed by 95% ethanol for a minimum of 24 h at room temperature. Fixed eyes were embedded in paraffin, and 4 μm sections were immuno-stained using the standard protocol. For DAB staining, sections were treated with 3% H_2O_2 in PBS (pH 11.95) for 60 min to bleach melanin. Subsequently, antigen retrieval was performed by heating in the presence of 10mM citric buffer (pH 6) in a pressure cooker set in a microwave oven for 10min. Subsequently, the sections were incubated with primary and HRP tagged secondary antibodies (Dako, USA), washed with 1X TBS, and developed using the DAB substrate (Vector Labs, USA). Following counterstaining with hematoxylin, the sections were mounted in permount and observed. For immunostaining with fluorescent secondary antibodies, deparaffinized and rehydrated sections were subjected to antigen retrieval by heating to 97°C in the presence of 25mM tris-1mM EDTA (pH 8.5) for 40 min [63]. Subsequently, sections were blocked in 1% BSA, washed, and incubated with the desired primary and secondary antibodies. The nuclei were stained with Hoechst (# 33342, Invitrogen, USA) and the sections mounted in Fluoromount-G (Southern Biotech, USA). Images were captured using a Leica inverted microscope (DMi8). A similar procedure was used for immunostaining cells cultured on cover-slips except that the antigen-retrieval step was omitted.

Uptake of rhodamine-Tf

RPE cells cultured on coverslips were incubated with rhodamine-tagged transferrin (20μM) in PBS for 5 min, rinsed 3–4 times with PBS, and chased in complete DMEM for 30 min before fixing in 4% paraformaldehyde. Coverslips were mounted and imaged as above.

Exposure to iron

RPE cells cultured on cover-slips in complete DMEM were exposed to 10μM ferrous ascorbate (Fe^{2+}), 10μM ferric ammonium citrate (FAC) (Fe^{3+}), or 100μM desferrioxamine (DFO) for 18h at 37°C. Control cells received an equal volume of vehicle. Subsequently, the cells were rinsed in PBS and immunostained with antibodies specific for α-syn and TfR.

In-vivo iron uptake

Equal counts of ^{59}Fe-citrate diluted in normal saline were introduced in the venous circulation of age and sex-matched α-syn$^{+/+}$ and α-syn$^{-/-}$ mice. Retro-orbital route that provides access to the nasal sinus was used instead of the customary tail vein to ensure equal introduction of ^{59}Fe in all animals. This was confirmed by counting ^{59}Fe in equal volume of

blood, and by fractionating equal volume of plasma on a native gel followed by autoradiography.

The animals were euthanized at indicated time points, blood was collected by cardiac puncture, organs were flushed with isotonic PBS in situ, and harvested. After rinsing in cold PBS, incorporation of ^{59}Fe was measured in a γ-counter (Beckman Gamma 5500). To evaluate uptake of ^{59}Fe by the eye, only the contra-lateral eye (*not used for injection*) was used. Uptake of ^{59}Fe by each organ was represented as per unit weight. Under these experimental conditions, uptake of ^{59}Fe by each mouse (carcass + blood + organs) was similar.

Isolation of the neuroretina

Freshly enucleated eyes from euthanized mice were incubated with 1% dispase at 37°C for 45min, and the neuroretina was scraped off under a light dissecting microscope. Isolated tissue was immediately processed for Western blotting.

Statistical analysis

Data were analyzed using GraphPad Prism5 software (GraphPad Software, Inc., La Jolla, CA) and presented as Mean ± SEM. Level of significance was calculated by unpaired t-test between the control and experimental.

Results

The neuroretina of α-syn$^{-/-}$ mice shows a phenotype of iron deficiency

To evaluate whether α-syn influences retinal iron homeostasis (Schematic 1), expression of TfR and ferritin, proteins necessary for the uptake and storage of iron respectively, was assessed in the neuroretina of α-syn$^{-/-}$ mice relative to α-syn$^{+/+}$ controls. Retinal sections were immunostained with specific antibodies to evaluate their distribution in situ, and neuroretinal lysates prepared from freshly harvested eyes were subjected to Western blotting to quantify the expression level. Immunoreaction for α-syn revealed prominent reaction in α-syn$^{+/+}$ samples in all layers of the neuroretina, including the RPE cell monolayer [19]. In the latter, expression of α-syn was more prominent on the BL membrane with minor punctate staining in intracellular compartments (Fig. 1A, panels 1 & 5). Retinal sections from α-syn$^{-/-}$ mice processed in parallel revealed no reaction for α-syn as expected (Fig. 1A, panels 2 & 6).

Immunoreaction for TfR showed a positive reaction in all layers of the neuroretina as reported previously [50]. In RPE cells, the reaction was more prominent on the BL membrane (Fig. 1B, panels 3 & 7). Surprisingly, the reaction for TfR was significantly lower in α-syn$^{-/-}$ samples in all layers of the neuroretina and the RPE cell monolayer relative to α-syn$^{+/+}$ controls (Fig. 1B, panels 3 & 7 vs 4 & 8). A similar evaluation for ferritin revealed prominent reactivity in all layers of the neuroretina including the RPE cell monolayer (Fig 2 A, panels 1 & 2). However, as observed for TfR, the reaction for ferritin was significantly reduced in the neuroretina and RPE cell monolayer of α-syn$^{-/-}$ samples relative to α-syn$^{+/+}$ controls (Fig. 2 A, panel 1 vs 2).

Further confirmation of downregulation of TfR and ferritin in α-syn$^{-/-}$ samples was obtained by fractionating neuroretinal lysates isolated from the eyes of α-syn$^{+/+}$and α-syn$^{-/-}$ mice by SDS-PAGE followed by Western blotting. Probing of transferred proteins for TfR and ferritin showed 5-fold downregulation of TfR and 3-fold downregulation of ferritin in α-syn$^{-/-}$ samples relative to α-syn$^{+/+}$ controls (Fig 2 B, lanes 1–3 vs 4–6, Fig. 2 C). Re-probing of the same membrane for RPE65, a retinal protein, and α-syn confirmed that the samples are representative of the neuroretina from α-syn$^{+/+}$ and α-syn$^{-/-}$ mice (Fig 2 B, lanes 1–3 vs 4–6).

Downregulation of ferritin in the neuroretina of α-syn$^{-/-}$ mice suggests depletion of iron stores and a phenotype of relative iron deficiency in the absence of α-syn. However, concomitant down-regulation of TfR was puzzling because iron deficiency normally up-regulates the expression of iron uptake proteins including the TfR. Subsequent experiments were therefore directed at resolving this dichotomy.

α-syn$^{-/-}$ mice show a phenotype of iron deficiency in the brain and hematopoietic organs

To evaluate whether the iron deficiency in α-syn$^{-/-}$ mice is limited to the neuroretina or more generalized, uptake of intravenously introduced radiolabeled iron ($^{59}FeCl_3$) by different organs of α-syn$^{-/-}$ mice was compared with α-syn$^{+/+}$ controls after 1 and 24 hours. Since almost all of ^{59}Fe introduced by this method is associated with plasma transferrin (Tf) (Supplemental Fig. 1), incorporation of ^{59}Fe provides an accurate estimate of the uptake of Tf-Fe by each organ during a specific time-period. Both mouse lines showed significantly higher ^{59}Fe counts in the spleen and femur at both time-points, organs that utilize significant amounts of Tf-Fe for hematopoiesis, relative to the liver and kidney that store excess circulating iron and re-absorb iron from the glomerular filtrate respectively [64, 65] (Fig 3 A & 3 B). Notably, uptake of ^{59}Fe by α-syn$^{-/-}$ spleen was significantly higher after 1 hour and fell to less than 50% of α-syn$^{+/+}$ controls after 24 hours (Fig 3 A & 3 B). Likewise, uptake of ^{59}Fe-Tf by the eyeball of α-syn$^{-/-}$ mice was significantly higher than controls after 1 hour, though the 24 hour counts were close to background because of the relatively less incorporation of ^{59}Fe by the eye (Fig. 3 C).

Increased uptake of ^{59}Fe-Tf by the spleen, femur, and eyeball of α-syn$^{-/-}$ mice after 1 hour suggests a phenotype of relative iron deficiency in these organs. A significant fall in ^{59}Fe counts after 24 hours relative to controls reflects inefficient incorporation of ^{59}Fe in ferritin, a possibility that was explored further by analyzing the expression of ferritin in tissue homogenates of brain, spleen, and liver of age and sex-matched α-syn$^{+/+}$ and α-syn$^{-/-}$ mice by Western blotting. Probing for ferritin revealed a significant decrease in the brain and spleen of α-syn$^{-/-}$ mice relative to controls (Fig. 3 D & 3 F, lanes 1–3 vs 4–6; Fig 3 E & 3 G). Expression of TfR was also decreased in the brain tissue of α-syn$^{-/-}$ mice relative to controls as observed in the neuroretina (Fig. 3 D, lanes 1- vs 4–6). Liver samples, however, showed minimal change in ferritin expression (Fig. 3 H, lanes 1–3 vs 4–6, Fig. 3 I), reflecting the ^{59}Fe uptake results in Figures 3 A and 3 B above.

The above observations indicate that α-syn plays an important role in the uptake and utilization of Tf-Fe, the principal source of iron for hematopoiesis [66]. To verify this assumption further, incorporation of ^{59}Fe-Tf in red blood cell (RBC) hemoglobin (Hb) of α-

syn$^{-/-}$ was compared with α-syn$^{+/+}$ controls. Thus, lysates of washed RBCs were fractionated by native gel electrophoresis, and incorporation of ^{59}Fe in Hb was visualized by autoradiography. The signal for ^{59}Fe-Hb from α-syn$^{-/-}$ RBCs was significantly less than matched controls despite similar levels of ^{59}Fe-Tf in the plasma, indicating impaired incorporation in the absence of α-syn (Fig. 4 A, lanes 1–3 vs 4 & 5; Fig. 4 B). Western blotting of RBC lysates and spleen homogenates revealed 3-fold and 2.5-fold reduction in α- and β-globin levels in α-syn$^{-/-}$ samples relative to α-syn$^{+/+}$ controls (Fig. 4 C & 4 E, lanes 1–3 vs 4–6; Fig. 4 D & 4 F), indicating reduced synthesis of Hb in α-syn$^{-/-}$ mice probably due to limited availability of Tf-Fe.

α-syn modulates the expression of ferritin and TfR in RPE cells

As noted in Figures 1 and 2 above, levels of TfR and ferritin were significantly reduced in the neuroretina of α-syn$^{-/-}$ mice, including the RPE cell monolayer. To evaluate whether this change is directly related to α-syn expression, RPE cells were transfected with siRNA specific for α-syn or scrambled control, and lysates were analyzed by Western blotting. Probing for α-syn confirmed efficient down-regulation of α-syn under these experimental conditions (Fig. 5 A, lane 3). Re-probing for TfR and ferritin showed 4-fold reduction in the expression of TfR and 2-fold reduction in ferritin (Fig. 5 A, lanes 3 vs 1 & 2; Fig. 5 B). Over-expression of α-syn in RPE cells, on the other hand, resulted in 3.5-fold upregulation of TfR and 3.8-fold increase in ferritin expression relative to controls (Fig. 5 C, lanes 3 vs 1 & 2; Fig. 5 D).

Together, these observations leave little doubt that ferritin, an indicator of intracellular iron stores, is directly related to α-syn expression in RPE cells. When combined with the *in vivo* data indicating generalized down-regulation of ferritin in the neuroretina and hematopoietic organs of α-syn$^{-/-}$ mice, it is likely that α-syn regulates the uptake of Tf-Fe, perhaps by modulating the endocytosis of Tf-TfR complex as indicated in a previous report [25]. Since RPE cells regulate transport of iron from choroidal capillaries to the neuroretina, such an activity would explain the phenotype of iron-deficiency in the neuroretina of α-syn$^{-/-}$ mice. Subsequent studies were directed at understanding the role of α-syn in endocytosis and recycling of Tf/TfR complex, and possible cause of down-regulation of TfR despite the iron deficiency.

Exogenous iron increases membrane association and co-localization of α-syn with the TfR

To stimulate the endocytosis of Tf/TfR complex, RPE cells were exposed to ferric ammonium citrate (FAC) or vehicle for 18h, rinsed with PBS, and fixed. Immunostaining of untreated control cells for α-syn revealed membrane association and co-localization with TfR especially at the tips of neurite-like processes (Fig. 6 A, panels 1–3). Exposure to FAC increased membrane association of α-syn and co-localization with the TfR (Fig. 6 B, panels 1–3, arrow-heads), while culture in the presence of the iron chelator desferrioxamine (DFO) resulted in down-regulation of α-syn and almost no co-localization with the TfR (Fig 6 C, panels 1–3).

Surprisingly, knock-down of α-syn with siRNA resulted in the accumulation of TfR in peri-nuclear vesicles, indicating disruption of its normal recycling to the plasma membrane

(Figure 7 A, panels 1 & 2). TfR-rich vesicles did not co-localize with the lysosomal marker LAMP1 (data not shown), suggesting accumulation in common recycling endosomes (CREs), not lysosomes.

To confirm these observations further, RPE cells expressing α-syn or its disease-associated mutant α-syn A53T were exposed to rhodamine-tagged Tf (Tf-Rh) for30 min, washed to remove free Tf-Rh, and fixed before capturing images. In cells expressing α-syn, immunoreactivity for TfR was mostly detected in vesicles near the plasma membrane as expected (Fig. 7B, panel 1). In cells expressing mutant α-syn A53T, on the other hand, TfR-containing vesicles were clustered in the peri-nuclear region (Fig. 7 B, panel 2). This observation provides further evidence that functional α-syn is necessary for the recycling of TfR from CREs to the plasma membrane.

Together, these observations indicate that α-syn responds to changes in extracellular iron and facilitates endocytosis of Tf/TfR complex from the plasma membrane. Down-regulation of α-syn or mutant α-syn-A53T disrupts this function, resulting in the accumulation of TfR in CREs. Such a scenario would also interfere with the release of Fe from Tf and incorporation in ferritin, explaining the down-regulation of ferritin and TfR in the neuroretina and brain tissue of α-syn$^{-/-}$mice observed above.

α-syn does not influence the uptake of non-transferrin bound iron by RPE cells

Since α-syn has been reported to function as a ferrireductase in neuroblastoma cells [44], its role in the uptake of non-Tf-bound iron (NTBI) by RPE cells was checked by exposing α-syn-over-expressing cells to a source of ferrous (Fe^{2+}) (ferrous ascorbate) or ferric (Fe^{3+}) (FAC) iron, the latter requiring reduction by a membrane-bound FR before transport through divalent metal transporters ZIP14, ZIP8, or DMT1 [67, 68]. As expected, exposure to Fe^{2+} and Fe^{3+} up-regulated ferritin and down-regulated TfR to limit further uptake of iron (Fig. 8 A & 8 B). However, over-expression of α-syn did not facilitate the uptake of Fe^{3+} (Fig. 8 A & 8 B, lanes 3 vs 6) [44]. Untreated α-syn-expressing cells, however, showed upregulation of ferritin and TfR relative to vector-expressing controls as demonstrated in Figure 5 above (Fig. 8, lanes 1vs 4). Thus, α-syn promotes the uptake of Tf-Fe, not NTBI in RPE cells.

Discussion

We describe a novel function of α-syn in modulating the transport and recycling of Tf/TfR complex, thereby influencing the uptake of Tf-Fe by RPE cells and other cell types. Absence of α-syn in transgenic mouse models resulted in a phenotype of relative iron deficiency in the neuroretina, spleen, and Hb, sites that utilize Tf-Fe as their primary source of iron. Down-regulation of α-syn in human RPE47 cells resulted in the re-distribution of Tf/TfR complex to peri-nuclear CREs and multi vesicular bodies (MVBs), underscoring the significance of α-syn in facilitating the transport of Tf/TfR-containing vesicles to the plasma membrane [25]. These observations link the well-described function of α-syn in vesicular transport [28] to retinal iron homeostasis and possible implications for PD-associated ocular pathology.

Although ocular manifestations are a significant cause of morbidity in people suffering from PD, the underlying cause has remained elusive. Until recently, visual symptoms were attributed to side-effects of drugs used for the management of PD [8]. However, advances in our understanding of the physiological function(s) of α-syn and its wide-spread expression in the neuroretina warrant a re-evaluation of this concept. Our observations on α-syn$^{+/+}$ mice confirmed expression of α-syn in all layers of the neuroretina, including the RPE cell monolayer where it was more prominent on the BL membrane (Figure 1A). The liver, spleen, brain, and RBCs also showed significant expression, confirming the ubiquitous presence of α-syn in most organs. Deletion of α-syn resulted in down-regulated ferritin and TfR in the brain, spleen, and neuroretina, organs that utilize mainly the Tf/TfR pathway of iron uptake. Organs that incorporate significant amounts of NTBI *via* divalent metal transporters such as the liver showed minimal change (Figures 2 & 3). Our data on the uptake of ^{59}Fe-Tf by the spleen of α-syn$^{-/-}$ mice provided additional insight on the underlying mechanism. Thus, a spike in ^{59}Fe counts after 1 hour followed by a significant decline in 24 hours suggested impaired release and/or transport of Tf-iron to the cytosol for incorporation in ferritin (Figure 3). Reduced availability of cytosolic iron explains the reduction in ^{59}Fe-Hb and total Hb in α-syn$^{-/-}$ RBCs and spleen tissue observed in this study (Figure 4) [69], and impaired hematopoiesis in α-syn$^{-/-}$ mice described earlier [30]. The *hemoglobin deficit* mouse model is another example where defective recycling of the Tf/TfR complex from CREs results in reduced incorporation of iron in reticulocytes carrying the *hbd* mutation [70]. It is unlikely that α-syn influences the uptake of NTBI as indicated by our in *vitro* data where over-expression of α-syn did not promote the uptake of ferric iron (Figure 8).

Interestingly, downregulation of ferritin despite increased presence of iron has been described in the SN of PD cases [71, 72], suggesting that aggregation of α-syn reproduces some of the down-stream effects of its absence in α-syn$^{-/-}$ mice.

How might α-syn influence the uptake of iron by the Tf/TfR pathway? In polarized cells, TfR is sorted to the BL domain through well-defined sorting signals in its cytoplasmic domain [73]. In polarized RPE cells, however, TfR has been detected on the AP membrane as well [74]. Uptake of Tf-Fe is initiated by the binding of iron-loaded Tf to the TfR, followed by internalization of the complex in clathrin-coated vesicles. These join the AP or BL pool of early or sorting endosomes where the low pH favors release of iron from Tf, which is reduced by membrane-bound ferrireductase proteins and transported to the cytosol through divalent metal transporters such as DMT1. Recycling of iron-depleted Tf/TfR complex to the respective plasma membrane domain occurs directly from sorting endosomes (fast recycling loop), or after translocation to perinuclear CREs that are accessible to both AP and BL recycling plasma membrane proteins (slow recycling loop). CREs therefore function as endosomal hubs that connect endocytic and exocytic membrane trafficking. Recycling of the Tf/TfR from early endosomes and CREs is facilitated by the adapter protein AP-1B that, through its interaction with clathrin, sorts and directs Tf/TfR carrying vesicles to the BL domain [73, 75, 76]. Since RPE cells lack AP-1B, basolaterally internalized TfR is transported randomly from CREs to AP and BL recycling and sorting endosomes before final delivery to the plasma membrane, a process regulated by SNAP23/25, VAMP2, and Rab11 [77–80]. Interestingly, α-syn exists as an unfolded and

monomeric cytosolic form and a multimeric membrane-bound form that chaperones the SNARE complex assembly by interacting with VAMP2 [21–23]. α-Syn also interacts with clathrin and members of the Rab family of proteins, thus modulating several steps in the endocytic and exocytic vesicular pathways including vesicular export, docking, and fusion with the plasma membrane [24, 81–84]. A specific role of α-syn in modulating the trafficking of clathrin-coated vesicles carrying the NMDR and Tf/TfR complex as cargo has been described recently [25, 26], providing further insight into its role in vesicular trafficking (Figure 9, left panel shaded in blue). Other proteins such as HFE also influence iron uptake by the Tf/TfR pathway, but unlike α-syn that modulates vesicular trafficking, HFE regulates the binding of Tf-Fe to the TfR at the plasma membrane [85]. Their role in iron uptake by the Tf/TfR pathway is therefore distinct.

In light of the above information, our observations clarify the mechanism by which α-syn modulates the uptake of Tf-Fe by RPE cells. Down-regulation of α-syn in RPE cells caused 2-fold reduction in ferritin and 4-fold reduction in TfR expression (Figure 5), supporting our in vivo observations on α-syn$^{-/-}$ mice. Exogenous expression of α-syn, on the other hand, enhanced ferritin and TfR expression above steady state levels, suggesting a direct role of α-syn in modulating ferritin and TfR expression (Figure 5). This observation was surprising since depletion of ferritin is expected to up-regulate TfR expression to replenish cellular iron stores. Lack of such a response suggests degradation of TfR rather than down-regulation in the absence of α-syn. Increased membrane association and co-localization of α-syn with TfR in response to extracellular iron suggests an active role of α-syn in the endocytosis of Tf-Fe/TfR complex (Figure 6 B & C), perhaps by interacting with clathrin as described [25]. Depletion or lack of α-syn is therefore likely to reduce the endocytosis of such vesicles, resulting in the depletion of cellular iron stores. However, the surprising accumulation of TfR in peri-nuclear CREs and LAMP1-negative MVBs by down-regulating α-syn suggests disruption of the recycling of Tf/TfR complex to the plasma membrane. Although *ad hoc* AP sorting signals such as glycans are expected to sort the TfR to AP or BL vesicles destined for the plasma membrane in the absence of AP-1B, accumulation of TfR in CREs in cells where α-syn is down-regulated suggests that α-syn plays a dominant role in the sorting and exocytosis of Tf/TfR complex to the plasma membrane (Figure 7 A). Externally added rhodamine-conjugated Tf (Rh-Tf) accumulated in similar peri-nuclear CREs in cells expressing mutant α-syn A53T as opposed to its normal distribution in α-syn-expressing controls (Figure 7 B), supporting the above conclusion. The accumulation of TfR in LAMP1 negative MVBs suggests that α-syn mediates the fusion of MVBs with lysosomes and/or the plasma membrane for exosomal release [86], processes that are disrupted in its absence (Figure 9, right panel, white). The sequestration of Tf/TfR complex in CREs and MVBs therefore explains the phenotype of iron deficiency and the unexpected down-regulation of both ferritin and TfR in α-syn deficient cells. Partial redistribution of TfR from its BL localization to the cytosol of RPE cells in α-syn$^{-/-}$ retinal sections (Figure 1 B) provides confidence that these observations are not an artifact of the cell line. A similar phenotype of iron deficiency in the hematopoietic organs of α-syn$^{-/-}$ mice suggests that this role of α-syn is not limited to the RPE cells. The response of other iron regulatory proteins such as IRP1 and IRP2 to the iron deficiency in α-syn$^{-/-}$ mice is an interesting question that remains unanswered by our data.

In conclusion, we propose that cytosolic localization of α-syn in RPE cells provides the necessary flexibility to facilitate the endocytosis of Tf/TfR complex from the AP or BL domain, and recycle the complex from CREs back to the plasma membrane based on iron concentration in the extracellular milieu. A facilitative role of α-syn in the uptake of Tf-Fe is evident from the phenotype of iron deficiency in all organs that utilize Tf-Fe. This phenotype is more prominent in RPE cells that lack AP-1B, and α-syn takes over its function in sorting and recycling Tf/TfR containing vesicles to the plasma membrane. Our observations that both α-syn and TfR are expressed on the BL domain of RPE cells *in vivo* supports active transport of iron from the choroidal blood through this pathway. Reduced incorporation of ^{59}Fe-Tf in enucleated eyes and down-regulation of ferritin in the neuroretina of α-syn $^{-/-}$ mice support this conclusion. On the other hand, perinuclear accumulation of TfR in CREs by knocking-down α-syn suggests a role in the exocytosis of this complex to the plasma membrane. It is therefore likely that α-syn influences both the endocytic and exocytic arm of Tf/TfR recycling, thereby normalizing iron concentration on either domain of RPE cells. Since iron is critical for the synthesis of dopamine and critical components of the visual cycle, dysfunction of α-syn may explain the ocular pathology and visual symptoms associated with PD.

Supplementary Material

Refer to Web version on PubMed Central for supplementary material.

Acknowledgments

This work was supported by NIH grants NS077438 and NS092145 to NS.

Abbreviations

α-syn	alpha synuclein
Tf	transferrin
TfR	transferrin receptor
DA	dopamine
PD	Parkinson’s disease
Tf-Fe	transferrin bound iron
NTBI	non transferrin bound iron
SN	substantia nigra
RPE	retinal pigment epithelium
OCT	optical coherence tomography
AMD	age related macular degeneration
Fpn	ferroportin

Hp	hephaestin
Cp	ceruloplasmin
ZIP	ZRT-IRT like protein
ZRT	Zinc regulatory transporter
IRT	Iron regulatory transporter
RLS	restless leg syndrome
FAC	ferric ammonium citrate
DFO	desferrioxamine
CRE	common recycling endosomes
MVB	multi vesicular body
AP	apical
BL	basolateral
TJ	tight junction
TGN	trans-Golgi network
SDS-PAGE	sodium dodecyl sulfate polyacrylamide gel electrophoresis

References

1. Stefanis L. alpha-Synuclein in Parkinson's disease. Cold Spring Harbor perspectives in medicine. 2012; 2(2):a009399. [PubMed: 22355802]
2. Shulman JM, De Jager PL, Feany MB. Parkinson's disease: genetics and pathogenesis. Annual review of pathology. 2011; 6:193–222.
3. Klein C, Westenberger A. Genetics of Parkinson's disease. Cold Spring Harbor perspectives in medicine. 2012; 2(1):a008888. [PubMed: 22315721]
4. Venda LL, Cragg SJ, Buchman VL, Wade-Martins R. alpha-Synuclein and dopamine at the crossroads of Parkinson's disease. Trends in neurosciences. 2010; 33(12):559–568. [PubMed: 20961626]
5. Cookson MR. alpha-Synuclein and neuronal cell death. Molecular neurodegeneration. 2009; 4:9. [PubMed: 19193223]
6. Sauerbier A, Jenner P, Todorova A, Chaudhuri KR. Non motor subtypes and Parkinson's disease. Parkinsonism & related disorders. 2016; 22(Suppl 1):S41–S46.
7. Archibald NK, Clarke MP, Mosimann UP, Burn DJ. The retina in Parkinson's disease. Brain : a journal of neurology. 2009; 132(Pt 5):1128–1145. [PubMed: 19336464]
8. Armstrong RA. Visual symptoms in Parkinson's disease. Parkinson's disease. 2011; 2011:908306.
9. Chorostecki J, Seraji-Bozorgzad N, Shah A, Bao F, Bao G, George E, Gorden V, Caon C, Frohman E, Tariq Bhatti M, Khan O. Characterization of retinal architecture in Parkinson's disease. Journal of the neurological sciences. 2015; 355(1–2):44–48. [PubMed: 26071887]
10. Bodis-Wollner I, Miri S, Glazman S. Venturing into the no-man's land of the retina in Parkinson's disease. Movement disorders : official journal of the Movement Disorder Society. 2014; 29(1):15–22. [PubMed: 24339212]

11. Garcia-Martin E, Satue M, Otin S, Fuertes I, Alarcia R, Larrosa JM, Polo V, Pablo LE. Retina measurements for diagnosis of Parkinson disease. Retina. 2014; 34(5):971–980. [PubMed: 24172914]
12. Jimenez B, Ascaso FJ, Cristobal JA, Lopez del Val J. Development of a prediction formula of Parkinson disease severity by optical coherence tomography. Movement disorders : official journal of the Movement Disorder Society. 2014; 29(1):68–74. [PubMed: 24458320]
13. Archibald NK, Clarke MP, Mosimann UP, Burn DJ. Retinal thickness in Parkinson's disease. Parkinsonism & related disorders. 2011; 17(6):431–436. [PubMed: 21454118]
14. Virgili G, Menchini F, Casazza G, Hogg R, Das RR, Wang X, Michelessi M. Optical coherence tomography (OCT) for detection of macular oedema in patients with diabetic retinopathy. The Cochrane database of systematic reviews. 2015; 1:CD008081. [PubMed: 25564068]
15. Keane PA, Mand PS, Liakopoulos S, Walsh AC, Sadda SR. Accuracy of retinal thickness measurements obtained with Cirrus optical coherence tomography. The British journal of ophthalmology. 2009; 93(11):1461–1467. [PubMed: 19574239]
16. Nguyen-Legros J. Functional neuroarchitecture of the retina: hypothesis on the dysfunction of retinal dopaminergic circuitry in Parkinson's disease. Surgical and radiologic anatomy : SRA. 1988; 10(2):137–144. [PubMed: 3135618]
17. Tatton WG, Kwan MM, Verrier MC, Seniuk NA, Theriault E. MPTP produces reversible disappearance of tyrosine hydroxylase-containing retinal amacrine cells. Brain research. 1990; 527(1):21–31. [PubMed: 1980839]
18. Popova E. Role of dopamine in distal retina. Journal of comparative physiology. A, Neuroethology, sensory, neural, and behavioral physiology. 2014; 200(5):333–358.
19. Martinez-Navarrete GC, Martin-Nieto J, Esteve-Rudd J, Angulo A, Cuenca N. Alpha synuclein gene expression profile in the retina of vertebrates. Molecular vision. 2007; 13:949–961. [PubMed: 17653035]
20. Lashuel HA, Overk CR, Oueslati A, Masliah E. The many faces of alpha-synuclein: from structure and toxicity to therapeutic target. Nature reviews. Neuroscience. 2013; 14(1):38–48.
21. Burre J, Sharma M, Tsetsenis T, Buchman V, Etherton MR, Sudhof TC. Alpha-synuclein promotes SNARE-complex assembly in vivo and in vitro. Science. 2010; 329(5999):1663–1667. [PubMed: 20798282]
22. Burre J, Sharma M, Sudhof TC. Definition of a molecular pathway mediating alpha-synuclein neurotoxicity. The Journal of neuroscience : the official journal of the Society for Neuroscience. 2015; 35(13):5221–5232. [PubMed: 25834048]
23. Burre J. The Synaptic Function of alpha-Synuclein. Journal of Parkinson's disease. 2015; 5(4):699–713.
24. Chutna O, Goncalves S, Villar-Pique A, Guerreiro P, Marijanovic Z, Mendes T, Ramalho J, Emmanouilidou E, Ventura S, Klucken J, Barral DC, Giorgini F, Vekrellis K, Outeiro TF. The small GTPase Rab11 co-localizes with alpha-synuclein in intracellular inclusions modulates its aggregation secretion and toxicity. Human molecular genetics. 2014; 23(25):6732–6745. [PubMed: 25092884]
25. Ben Gedalya T, Loeb V, Israeli E, Altschuler Y, Selkoe DJ, Sharon R. Alpha-synuclein and polyunsaturated fatty acids promote clathrin-mediated endocytosis and synaptic vesicle recycling. Traffic. 2009; 10(2):218–234. [PubMed: 18980610]
26. Cheng F, Li X, Li Y, Wang C, Wang T, Liu G, Baskys A, Ueda K, Chan P, Yu S. alpha-Synuclein promotes clathrin-mediated NMDA receptor endocytosis and attenuates NMDA-induced dopaminergic cell death. Journal of neurochemistry. 2011; 119(4):815–825. [PubMed: 21883224]
27. Perez RG, Waymire JC, Lin E, Liu JJ, Guo F, Zigmond MJ. A role for alpha-synuclein in the regulation of dopamine biosynthesis. The Journal of neuroscience : the official journal of the Society for Neuroscience. 2002; 22(8):3090–3099. [PubMed: 11943812]
28. Bendor JT, Logan TP, Edwards RH. The function of alpha-synuclein. Neuron. 2013; 79(6):1044–1066. [PubMed: 24050397]
29. Abeliovich A, Schmitz Y, Farinas I, Choi-Lundberg D, Ho WH, Castillo PE, Shinsky N, Verdugo JM, Armanini M, Ryan A, Hynes M, Phillips H, Sulzer D, Rosenthal A. Mice lacking alpha-

synuclein display functional deficits in the nigrostriatal dopamine system. Neuron. 2000; 25(1): 239–252. [PubMed: 10707987]

30. Xiao W, Shameli A, Harding CV, Meyerson HJ, Maitta RW. Late stages of hematopoiesis and B cell lymphopoiesis are regulated by alpha-synuclein a key player in Parkinson's disease. Immunobiology. 2014; 219(11):836–844. [PubMed: 25092570]
31. Ho CY, Troncoso JC, Knox D, Stark W, Eberhart CG. Beta-amyloid, phospho-tau and alpha-synuclein deposits similar to those in the brain are not identified in the eyes of Alzheimer's and Parkinson's disease patients. Brain pathology. 2014; 24(1):25–32. [PubMed: 23714377]
32. Bodis-Wollner I, Kozlowski PB, Glazman S, Miri S. alpha-synuclein in the inner retina in parkinson disease. Annals of neurology. 2014; 75(6):964–966. [PubMed: 24816946]
33. Stover NP, Watts RL. Spheramine for treatment of Parkinson's disease. Neurotherapeutics : the journal of the American Society for Experimental NeuroTherapeutics. 2008; 5(2):252–259. [PubMed: 18394567]
34. Yin F, Tian ZM, Liu S, Zhao QJ, Wang RM, Shen L, Wieman J, Yan Y. Transplantation of human retinal pigment epithelium cells in the treatment for Parkinson disease. CNS neuroscience & therapeutics. 2012; 18(12):1012–1020. [PubMed: 23190934]
35. Ming M, Li X, Fan X, Yang D, Li L, Chen S, Gu Q, Le W. Retinal pigment epithelial cells secrete neurotrophic factors and synthesize dopamine: possible contribution to therapeutic effects of RPE cell transplantation in Parkinson's disease. Journal of translational medicine. 2009; 7:53. [PubMed: 19558709]
36. Brilliant MH, Vaziri K, Connor TB Jr, Schwartz SG, Carroll JJ, McCarty CA, Schrodi SJ, Hebbring SJ, Kishor KS, Flynn HW Jr, Moshfeghi AA, Moshfeghi DM, Fini ME, McKay BS. Mining Retrospective Data for Virtual Prospective Drug Repurposing: L-DOPA and Age-related Macular Degeneration. The American journal of medicine. 2016; 129(3):292–298. [PubMed: 26524704]
37. Sidhu A, Wersinger C, Vernier P. Does alpha-synuclein modulate dopaminergic synaptic content and tone at the synapse? FASEB journal : official publication of the Federation of American Societies for Experimental Biology. 2004; 18(6):637–647. [PubMed: 15054086]
38. Ayton S, Lei P. Nigral iron elevation is an invariable feature of Parkinson's disease and is a sufficient cause of neurodegeneration. BioMed research international. 2014; 2014:581256. [PubMed: 24527451]
39. Song D, Dunaief JL. Retinal iron homeostasis in health and disease. Frontiers in aging neuroscience. 2013; 5:24. [PubMed: 23825457]
40. Sian-Hulsmann J, Mandel S, Youdim MB, Riederer P. The relevance of iron in the pathogenesis of Parkinson's disease. Journal of neurochemistry. 2011; 118(6):939–957. [PubMed: 21138437]
41. Lee HP, Zhu X, Liu G, Chen SG, Perry G, Smith MA, Lee HG. Divalent metal transporter iron and Parkinson's disease: a pathological relationship. Cell research. 2010; 20(4):397–399. [PubMed: 20357807]
42. Lu Y, Prudent M, Fauvet B, Lashuel HA, Girault HH. Phosphorylation of alpha-Synuclein at Y125 and S129 alters its metal binding properties: implications for understanding the role of alpha-Synuclein in the pathogenesis of Parkinson's Disease and related disorders. ACS chemical neuroscience. 2011; 2(11):667–675. [PubMed: 22860160]
43. Peng Y, Wang C, Xu HH, Liu YN, Zhou F. Binding of alpha-synuclein with Fe(III) and with Fe(II) and biological implications of the resultant complexes. Journal of inorganic biochemistry. 2010; 104(4):365–370. [PubMed: 20005574]
44. Davies P, Moualla D, Brown DR. Alpha-synuclein is a cellular ferrireductase. PloS one. 2011; 6(1):e15814. [PubMed: 21249223]
45. Olivares D, Huang X, Branden L, Greig NH, Rogers JT. Physiological and pathological role of alpha-synuclein in Parkinson's disease through iron mediated oxidative stress; the role of a putative iron-responsive element. International journal of molecular sciences. 2009; 10(3):1226–1260. [PubMed: 19399246]
46. Febbraro F, Giorgi M, Caldarola S, Loreni F, Romero-Ramos M. alpha-Synuclein expression is modulated at the translational level by iron. Neuroreport. 2012; 23(9):576–580. [PubMed: 22581044]

47. Golts N, Snyder H, Frasier M, Theisler C, Choi P, Wolozin B. Magnesium inhibits spontaneous and iron-induced aggregation of alpha-synuclein. The Journal of biological chemistry. 2002; 277(18): 16116–16123. [PubMed: 11850416]
48. Paris I, Martinez-Alvarado P, Cardenas S, Perez-Pastene C, Graumann R, Fuentes P, Olea-Azar C, Caviedes P, Segura-Aguilar J. Dopamine-dependent iron toxicity in cells derived from rat hypothalamus. Chemical research in toxicology. 2005; 18(3):415–419. [PubMed: 15777081]
49. Funke C, Schneider SA, Berg D, Kell DB. Genetics and iron in the systems biology of Parkinson's disease and some related disorders. Neurochemistry international. 2013; 62(5):637–652. [PubMed: 23220386]
50. Garcia-Castineiras S. Iron, the retina and the lens: a focused review. Experimental eye research. 2010; 90(6):664–678. [PubMed: 20230820]
51. Lozoff B. Early iron deficiency has brain and behavior effects consistent with dopaminergic dysfunction. The Journal of nutrition. 2011; 141(4):740S–746S. [PubMed: 21346104]
52. Bianco LE, Wiesinger J, Earley CJ, Jones BC, Beard JL. Iron deficiency alters dopamine uptake and response to L-DOPA injection in Sprague-Dawley rats. Journal of neurochemistry. 2008; 106(1):205–215. [PubMed: 18363828]
53. Matak P, Matak A, Moustafa S, Aryal DK, Benner EJ, Wetsel W, Andrews NC. Disrupted iron homeostasis causes dopaminergic neurodegeneration in mice. Proceedings of the National Academy of Sciences of the United States of America. 2016; 113(13):3428–3435. [PubMed: 26929359]
54. Turjanski N, Lees AJ, Brooks DJ. Striatal dopaminergic function in restless legs syndrome: 18F–dopa and 11C–raclopride PET studies. Neurology. 1999; 52(5):932–937. [PubMed: 10102408]
55. Moiseyev G, Takahashi Y, Chen Y, Gentleman S, Redmond TM, Crouch RK, Ma JX. RPE65 is an iron(II)-dependent isomerohydrolase in the retinoid visual cycle. The Journal of biological chemistry. 2006; 281(5):2835–2840. [PubMed: 16319067]
56. He X, Hahn P, Iacovelli J, Wong R, King C, Bhisitkul R, Massaro-Giordano M, Dunaief JL. Iron homeostasis and toxicity in retinal degeneration. Progress in retinal and eye research. 2007; 26(6): 649–673. [PubMed: 17921041]
57. Goralska M, Ferrell J, Harned J, Lall M, Nagar S, Fleisher LN, McGahan MC. Iron metabolism in the eye: a review. Experimental eye research. 2009; 88(2):204–215. [PubMed: 19059397]
58. Newman, EA. Müller Cells and the Retinal Pigment Epithelium. In: Albert, DM.; Jakobiec, FA., editors. Principles and Practice of Ophthalmology. Philadelphia: W.B. Saunders Co; 1994. p. 398-419.
59. Lehmann GL, Benedicto I, Philp NJ, Rodriguez-Boulan E. Plasma membrane protein polarity and trafficking in RPE cells: past, present and future. Experimental eye research. 2014; 126:5–15. [PubMed: 25152359]
60. Leung KW, Liu M, Xu X, Seiler MJ, Barnstable CJ, Tombran-Tink J. Expression of ZnT and ZIP zinc transporters in the human RPE and their regulation by neurotrophic factors. Investigative ophthalmology & visual science. 2008; 49(3):1221–1231. [PubMed: 18326752]
61. Hunt RC, Davis AA. Release of iron by human retinal pigment epithelial cells. Journal of cellular physiology. 1992; 152(1):102–110. [PubMed: 1618912]
62. Del Monte MA, Rabbani R, Diaz TC, Lattimer SA, Nakamura J, Brennan MC, Greene DA. Sorbitol myo-inositol and rod outer segment phagocytosis in cultured hRPE cells exposed to glucose. In vitro model of myo-inositol depletion hypothesis of diabetic complications. Diabetes. 1991; 40(10):1335–1345. [PubMed: 1936595]
63. Theurl M, Song D, Clark E, Sterling J, Grieco S, Altamura S, Galy B, Hentze M, Muckenthaler MU, Dunaief JL. Mice with hepcidin-resistant ferroportin accumulate iron in the retina. FASEB journal : official publication of the Federation of American Societies for Experimental Biology. 2016; 30(2):813–823. [PubMed: 26506980]
64. Kohgo Y, Ikuta K, Ohtake T, Torimoto Y, Kato J. Body iron metabolism and pathophysiology of iron overload. International journal of hematology. 2008; 88(1):7–15. [PubMed: 18594779]
65. Rahman YE, Cerny EA, Lau EH, Carnes BA. Enhanced iron removal from liver parenchymal cells in experimental iron overload: liposome encapsulation of HBED and phenobarbital administration. Blood. 1983; 62(1):209–213. [PubMed: 6407548]

66. Li H, Ginzburg YZ. Crosstalk between Iron Metabolism and Erythropoiesis. Advances in hematology. 2010; 2010:605435. [PubMed: 20631898]

67. Wang CY, Jenkitkasemwong S, Duarte S, Sparkman BK, Shawki A, Mackenzie B, Knutson MD. ZIP8 is an iron and zinc transporter whose cell-surface expression is up-regulated by cellular iron loading. The Journal of biological chemistry. 2012; 287(41):34032–34043. [PubMed: 22898811]

68. Liuzzi JP, Aydemir F, Nam H, Knutson MD, Cousins RJ. Zip14 (Slc39a14) mediates non-transferrin-bound iron uptake into cells. Proceedings of the National Academy of Sciences of the United States of America. 2006; 103(37):13612–13617. [PubMed: 16950869]

69. Ponka P. Tissue-specific regulation of iron metabolism and heme synthesis: distinct control mechanisms in erythroid cells. Blood. 1997; 89(1):1–25. [PubMed: 8978272]

70. Garrick MD, Garrick LM. Loss of rapid transferrin receptor recycling due to a mutation in Sec15l1 in hbd mice. Biochimica et biophysica acta. 2007; 1773(2):105–108. [PubMed: 17087999]

71. Dexter DT, Carayon A, Javoy-Agid F, Agid Y, Wells FR, Daniel SE, Lees AJ, Jenner P, Marsden CD. Alterations in the levels of iron, ferritin and other trace metals in Parkinson's disease and other neurodegenerative diseases affecting the basal ganglia. Brain : a journal of neurology. 1991; 114(Pt 4):1953–1975. [PubMed: 1832073]

72. Connor JR, Snyder BS, Arosio P, Loeffler DA, LeWitt P. A quantitative analysis of isoferritins in select regions of aged parkinsonian and Alzheimer's diseased brains. Journal of neurochemistry. 1995; 65(2):717–724. [PubMed: 7616228]

73. Gravotta D, Carvajal-Gonzalez JM, Mattera R, Deborde S, Banfelder JR, Bonifacino JS, Rodriguez-Boulan E. The clathrin adaptor AP-1A mediates basolateral polarity. Developmental cell. 2012; 22(4):811–823. [PubMed: 22516199]

74. Ugarte M, Osborne NN, Brown LA, Bishop PN. Iron, zinc and copper in retinal physiology and disease. Survey of ophthalmology. 2013; 58(6):585–609. [PubMed: 24160731]

75. Odorizzi G, Trowbridge IS. Structural requirements for basolateral sorting of the human transferrin receptor in the biosynthetic and endocytic pathways of Madin-Darby canine kidney cells. The Journal of cell biology. 1997; 137(6):1255–1264. [PubMed: 9182660]

76. Gonzalez A, Rodriguez-Boulan E. Clathrin and AP1B: key roles in basolateral trafficking through trans-endosomal routes. FEBS letters. 2009; 583(23):3784–3795. [PubMed: 19854182]

77. Perez Bay AE, Schreiner R, Benedicto I, Rodriguez-Boulan EJ. Galectin-4-mediated transcytosis of transferrin receptor. Journal of cell science. 2014; 127(Pt 20):4457–4469. [PubMed: 25179596]

78. Perez Bay AE, Schreiner R, Mazzoni F, Carvajal-Gonzalez JM, Gravotta D, Perret E, Lehmann Mantaras G, Zhu YS, Rodriguez-Boulan EJ. The kinesin KIF16B mediates apical transcytosis of transferrin receptor in AP-1B–deficient epithelia. The EMBO journal. 2013; 32(15):2125–2139. [PubMed: 23749212]

79. Kubo K, Kobayashi M, Nozaki S, Yagi C, Hatsuzawa K, Katoh Y, Shin HW, Takahashi S, Nakayama K. SNAP23/25 and VAMP2 mediate exocytic event of transferrin receptor-containing recycling vesicles. Biology open. 2015; 4(7):910–920. [PubMed: 26092867]

80. Takahashi S, Kubo K, Waguri S, Yabashi A, Shin HW, Katoh Y, Nakayama K. Rab11 regulates exocytosis of recycling vesicles at the plasma membrane. Journal of cell science. 2012; 125(Pt 17): 4049–4057. [PubMed: 22685325]

81. Gitler AD, Bevis BJ, Shorter J, Strathearn KE, Hamamichi S, Su LJ, Caldwell KA, Caldwell GA, Rochet JC, McCaffery JM, Barlowe C, Lindquist S. The Parkinson's disease protein alpha-synuclein disrupts cellular Rab homeostasis. Proceedings of the National Academy of Sciences of the United States of America. 2008; 105(1):145–150. [PubMed: 18162536]

82. Eisbach SE, Outeiro TF. Alpha-synuclein and intracellular trafficking: impact on the spreading of Parkinson's disease pathology. Journal of molecular medicine. 2013; 91(6):693–703. [PubMed: 23616088]

83. Chua CE, Tang BL, Rabs. SNAREs and alpha-synuclein--membrane trafficking defects in synucleinopathies. Brain research reviews. 2011; 67(1–2):268–281. [PubMed: 21439320]

84. Vargas KJ, Makani S, Davis T, Westphal CH, Castillo PE, Chandra SS. Synucleins regulate the kinetics of synaptic vesicle endocytosis. The Journal of neuroscience : the official journal of the Society for Neuroscience. 2014; 34(28):9364–9376. [PubMed: 25009269]

85. Pelham C, Jimenez T, Rodova M, Rudolph A, Chipps E, Islam MR. Regulation of HFE expression by poly(ADP-ribose) polymerase-1 (PARP1) through an inverted repeat DNA sequence in the distal promoter. Biochimica et biophysica acta. 2013; 1829(12):1257–1265. [PubMed: 24184271]

86. Fader CM, Colombo MI. Autophagy and multi vesicular bodies: two closely related partners. Cell death and differentiation. 2009; 16(1):70–78. [PubMed: 19008921]

Highlights

1. α-Synuclein promotes transferrin-mediated iron uptake.
2. Absence of α-synuclein disrupts the recycling of Tf/TfR complex.
3. α-Synuclein maintains retinal iron homeostasis.
4. Dysfunction of α-synuclein could contribute to the visual symptoms of PD.

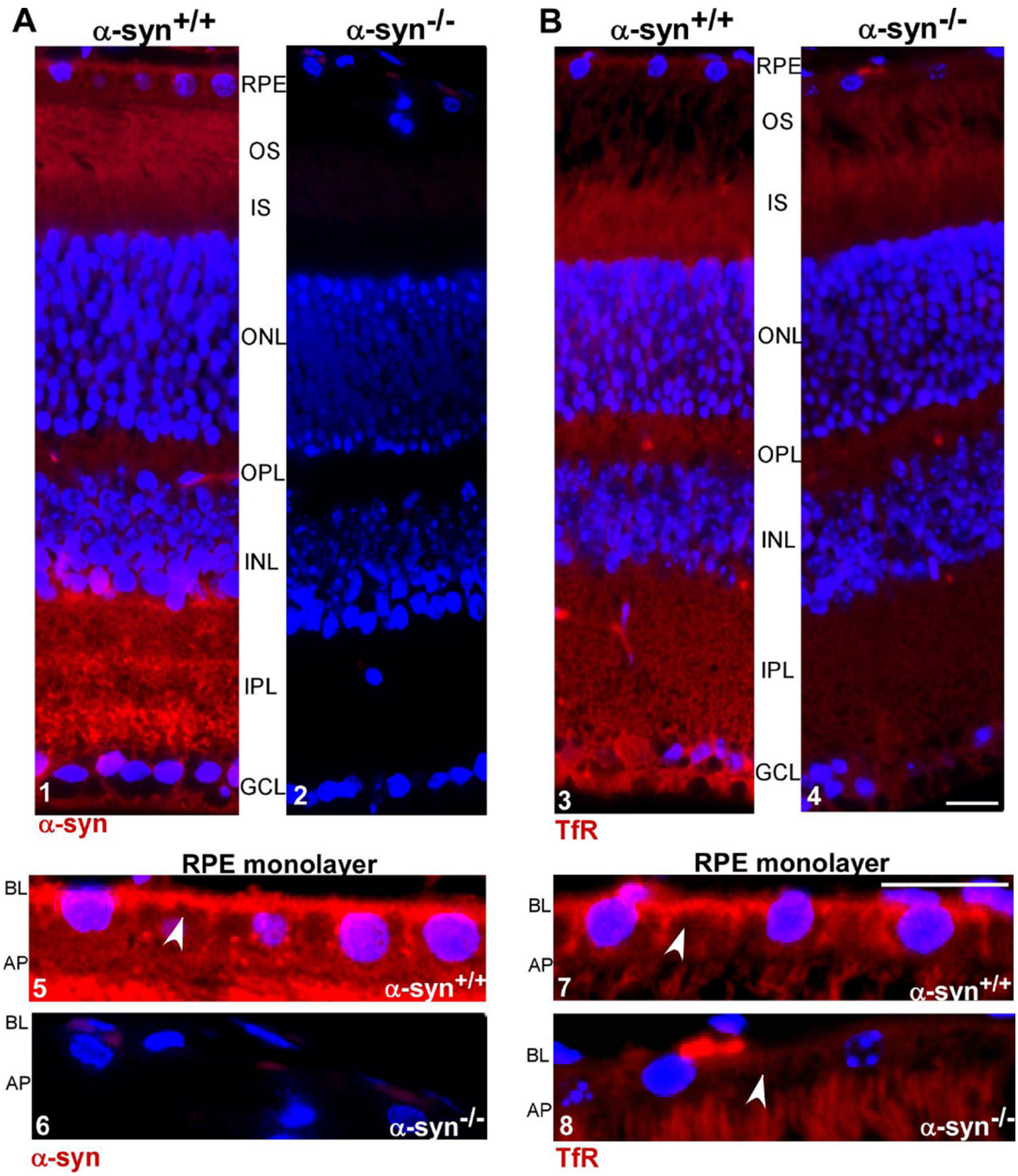

Figure 1. α-syn and TfR are localized to the BL domain of RPE cells in retinal sections

(A) Retinal sections from α-syn$^{+/+}$ mice show positive immunoreaction for α-syn in all retinal cell layers. In RPE cell monolayer the reaction is more prominent on the BL domain (panels 1 & 5). Sections from α-syn$^{-/-}$ mice show no reactivity for α-syn as expected (panels 2 & 6). **(B)** A positive immunoreactivity for TfR is detected in all layers of the retina from α-syn$^{+/+}$ and α-syn$^{-/-}$mice (panels 3, 4, 7, 8). Notably, the reaction is more prominent on the BL membrane of RPE cells (panel 7) and is significantly lower in α-syn$^{-/-}$ samples relative to α-syn$^{+/+}$ controls (panels 3 & 7 vs 4 & 8). RPE: retinal pigment epithelium; OS:

outer segment of photoreceptor layer; IS: inner segment of photoreceptor layer; ONL: outer nuclear layer; OPL: outer plexiform layer; INL: inner nuclear layer; IPL: inner plexiform layer; GCL: ganglion cell layer. Scale bar 10μm.

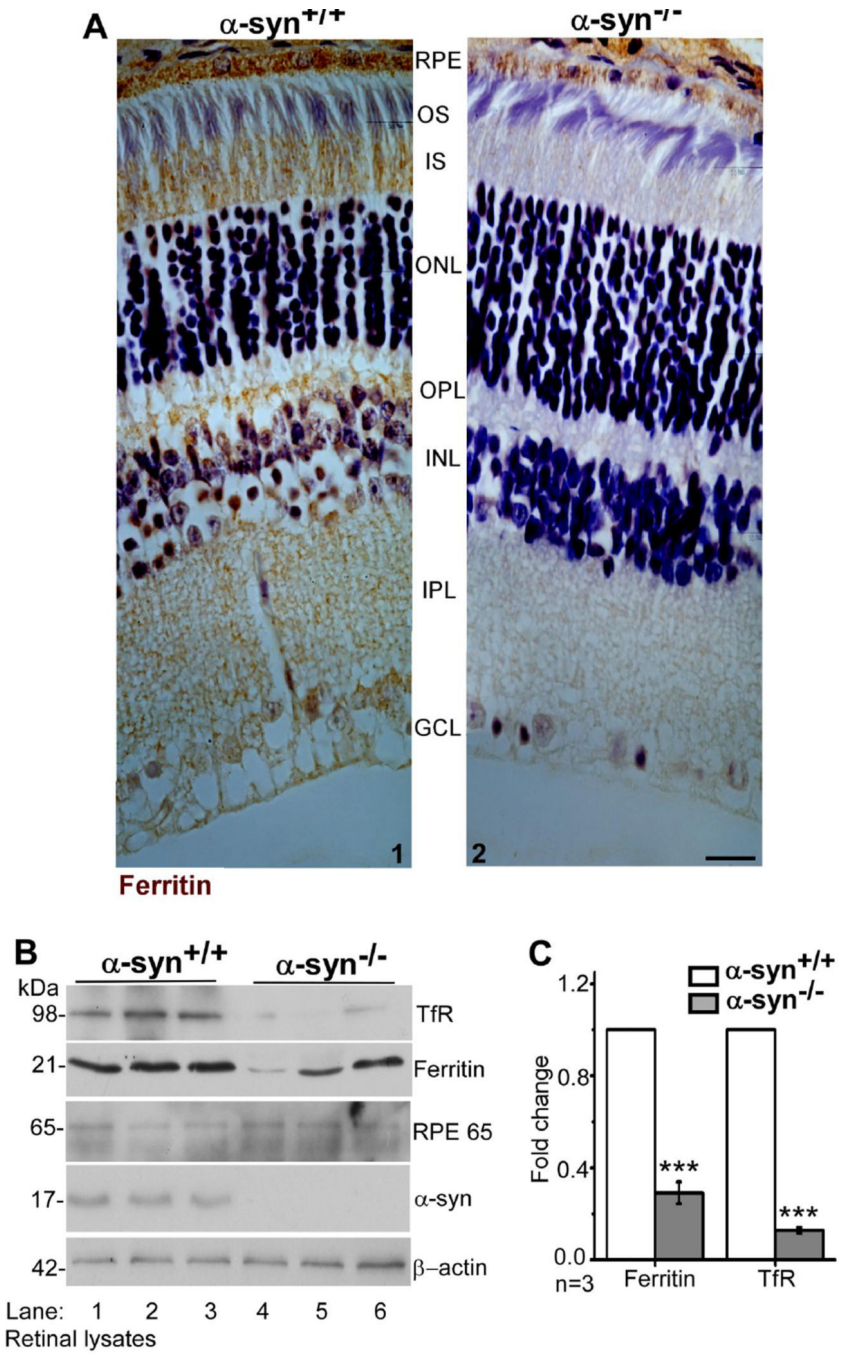

Figure 2. Ferritin and TfR are downregulated in the neuroretina of α-syn$^{-/-}$ mice

(A) Immunoreaction for ferritin is significantly reduced in all layers of the retina from α-syn$^{-/-}$ mice relative to α-syn$^{+/+}$ controls, including the RPE cell monolayer (panels 2 vs 1). Scale bar 10μm. **(B)** Probing of neuroretinal lysates harvested from α-syn$^{-/-}$ mice with specific antibodies shows significant down-regulation of ferritin and TfR relative to α-syn$^{+/+}$ controls (lanes 1–3 vs 4–6). Reactivity for the retinal marker RPE65 is positive in all samples and reactivity for α-syn is limited to α-syn$^{+/+}$ samples as expected (lanes 1–6). **(C)** Quantification by densitometry shows 5-fold decrease in TfR and 3-fold decrease in ferritin

in α-syn$^{-/-}$ samples relative to controls. (n=3; ***p<0.001). Values are mean ± SEM of the indicated *n*. All values were normalized to β-actin that served as an internal control.

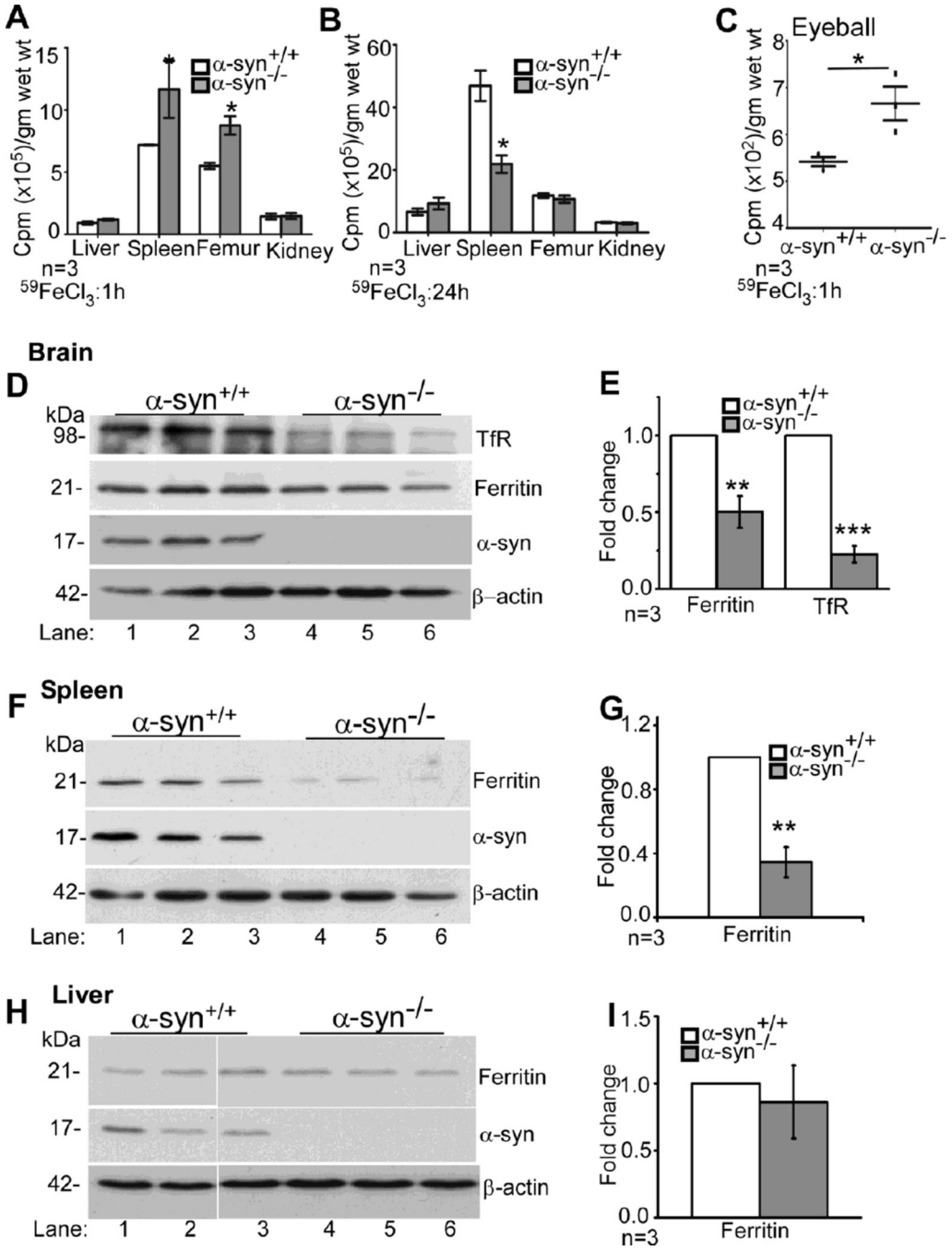

Figure 3. α-Syn$^{-/-}$ mice are iron deficient

(A–C) Age and sex-matched α-syn$^{-/-}$ and α-syn$^{+/+}$ mice were injected with $^{59}FeCl_3$ intravenously and sacrificed after 1 or 24 hours. Tf-^{59}Fe counts in the spleen and femur of α-syn$^{-/-}$ mice are significantly higher than α-syn$^{+/+}$ controls after 1 hour, and 2-fold reduced compared to the control value after 24 hours especially in the spleen. Likewise, Tf-^{59}Fe counts in the enucleated eyeball of α-syn$^{-/-}$ mice are significantly higher than α-syn$^{+/+}$ controls after 1 hour. (^{59}Fe counts in each organ were normalized to plasma counts in the respective mice). (n=3; $^{**}p<0.01$, $^{*}p<0.05$). **(D & E)** Probing of brain lysates from α-

syn$^{-/-}$ mice with specific antibodies shows 2-fold decrease in ferritin and 4-fold decrease in TfR levels relative to α-syn$^{+/+}$ controls. Reactivity for α-syn is as expected (lanes 1–3 vs 4–6). **(F–I)** A similar evaluation of spleen and liver tissue lysates from α-syn$^{-/-}$ mice shows 2.5-fold reduction in spleen ferritin and no change in liver ferritin relative to α-syn$^{+/+}$ controls (lanes 1–3 vs 4–6). β-actin served as an internal control for quantification by densitometry. (n=3; values are mean ± SEM of the indicated *n*. **p*<0.05, ***p*<0.01, *** *p*<0.001. Note: lysates in panel H were fractionated on the same gel and rearranged using Adobe Photoshop.

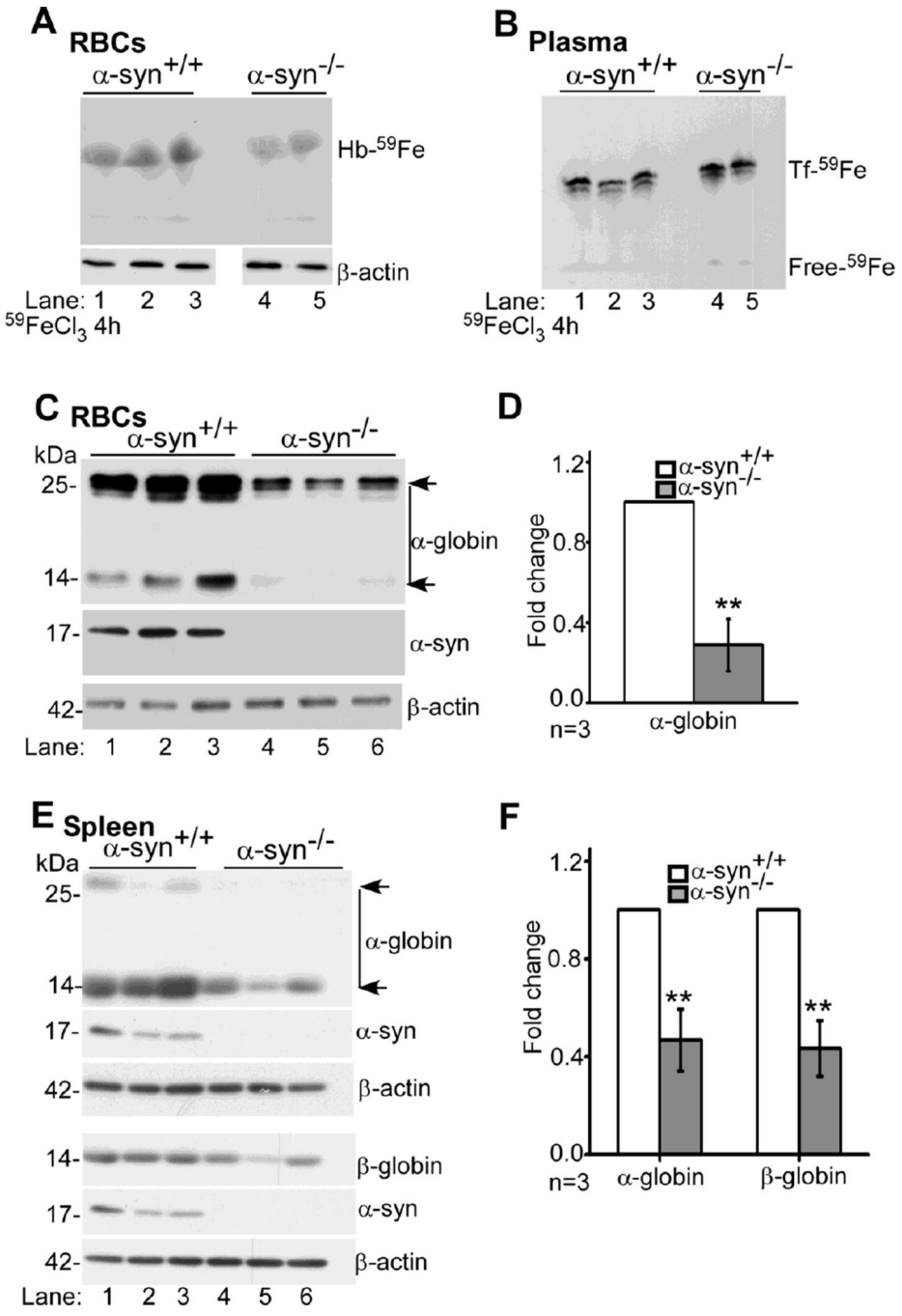

Figure 4. α-Syn$^{-/-}$ mice show impaired hematopoiesis

(A & B) Age and sex-matched α-syn$^{-/-}$and α-syn$^{+/+}$ mice were injected with $^{59}FeCl_3$ intravenously and sacrificed after 4 hours. RBCs and plasma separated from harvested blood were fractionated by native gel electrophoresis, and incorporation of ^{59}Fe in Hb and Tf was quantified by autoradiography. Equal volume of each sample was analyzed by Western blotting and probed for β-actin. The signal for ^{59}Fe-Hb in α-syn$^{-/-}$ samples is significantly lower than matched α-syn$^{+/+}$ controls (A, lanes 1–3 vs 4,5). The signal for ^{59}Fe-Tf, however, is slightly higher in α-syn$^{-/-}$ samples relative to controls (B, lanes 1–3 vs 4,5). **(C–**

F) Lysates prepared from washed RBCs and spleen tissue from age- and sex-matched α-syn$^{+/+}$ and α-syn$^{-/-}$ mice were analyzed by Western blotting. Probing for α-globin and β-globin on separate gels reveals 3-fold reduction in α-globin expression in α-syn$^{-/-}$ RBCs (C, lanes 1–3 vs 4–6; D) and 2.5-fold reduction in α-globin and β-globin in α-syn$^{-/-}$ spleen tissue relative to controls (E, lanes 1–3 vs 4–6, F). Reaction for β-actin served as an internal control for quantification by densitometry. (n=3; $^{**}p<0.01$). Values are mean ± SEM of the indicated *n*.

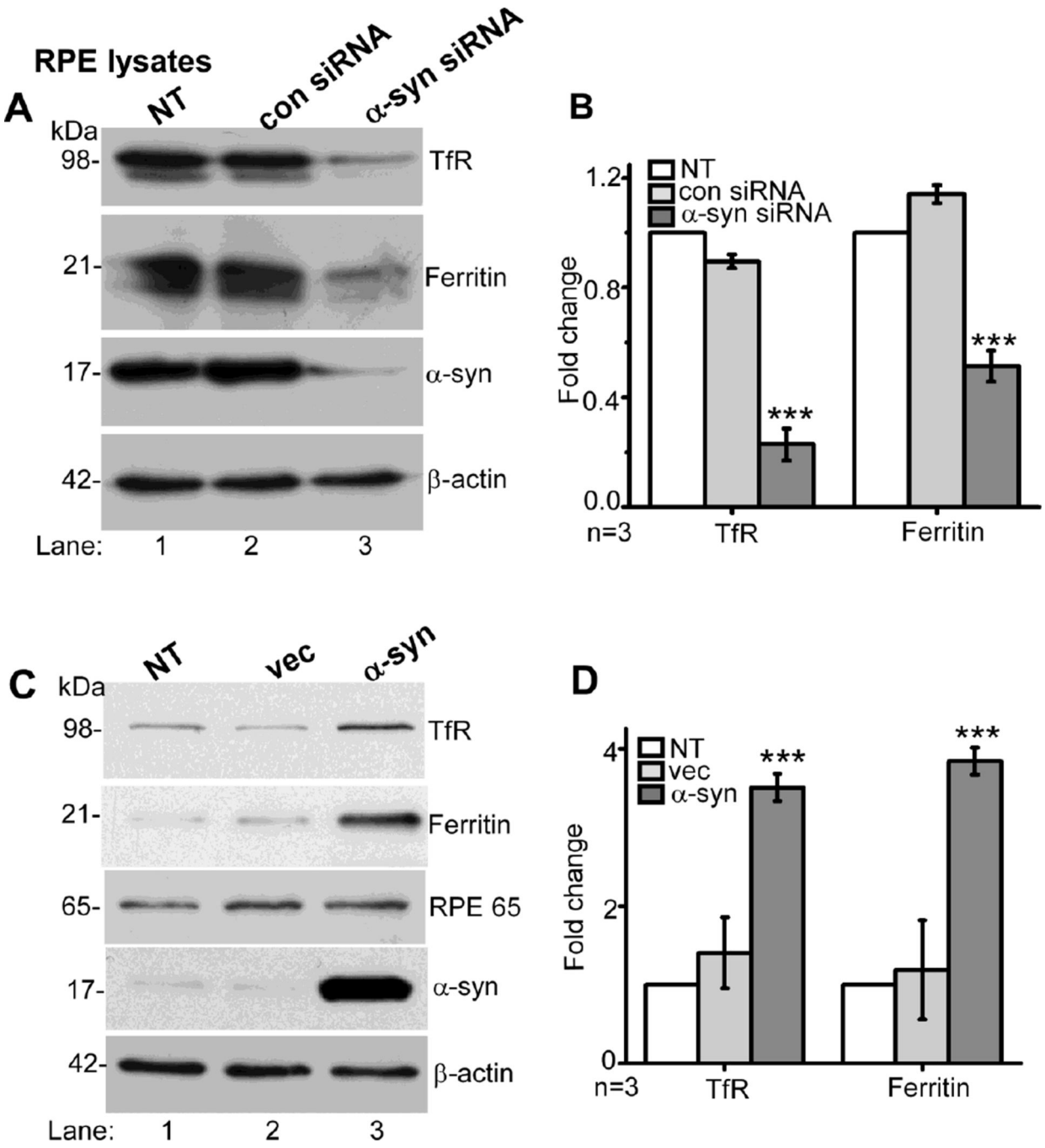

Figure 5. α-Syn modulates the expression of TfR and ferritin in cultured RPE cells

(A & B) Lysates prepared from RPE cells transfected with siRNA for α-syn, control siRNA, and non-transfected controls were analyzed by Western blotting. Probing with specific antibodies shows 90% reduction in α-syn in cells transfected with α-syn siRNA as expected (A, lane 3 vs 1, 2). Notably, knock-down of α-syn results in 4-fold reduction in TfR and 2-fold reduction in ferritin relative to controls (lane 3 vs 1, 2; B). **(C & D)** Over-expression of α-syn in RPE cells results in 3.5-fold increase in TfR and 3.8-fold increase in ferritin expression relative to non-transfected and vector-transfected controls (C, lane 3 vs 1, 2; D).

(n=3; ***$p<0.001$). Reaction for β-actin served as an internal control for protein loading in panels A and C. Values are mean ± SEM of the indicated *n*.

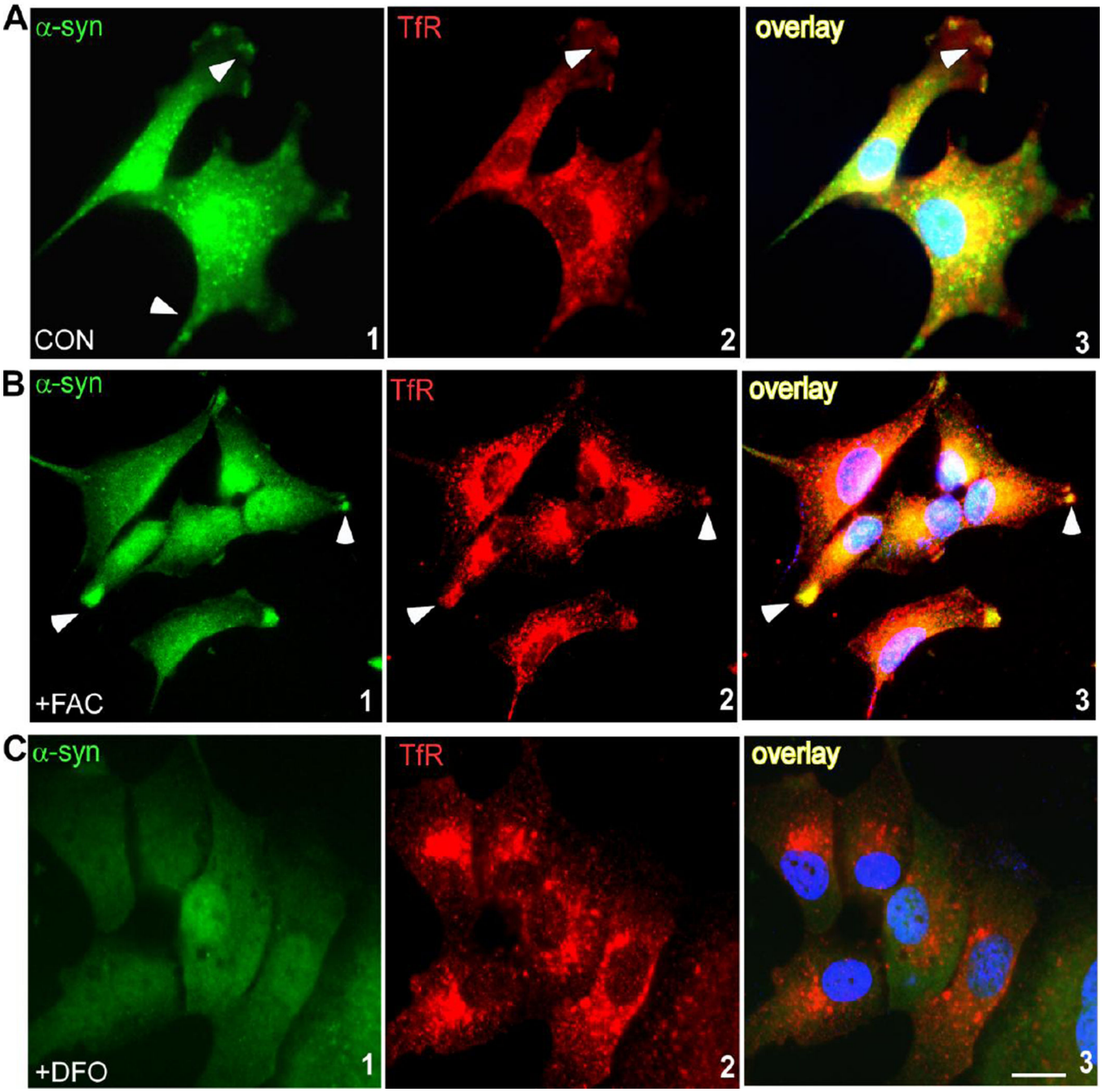

Figure 6. Exposure of RPE cells to iron increases membrane association and co-localization of α-syn with the TfR

(A) Endogenous α-syn (green) in RPE cells is distributed between the membrane and intracellular compartments (panel 1), and co-localizes with the TfR (red) at the membrane (panels 2 & 3). **(B)** Exposure to iron increases membrane association and co-localization of α-syn with the TfR (panels 1–3). FAC: ferric ammonium citrate. **(C)** Exposure of RPE cells to DFO results in down-regulation of α-syn (panel 1), re-distribution of TfR from the plasma membrane (panel 2), and minimal co-localization of α-syn with the TfR (panel 3). Scale bar 10μm.

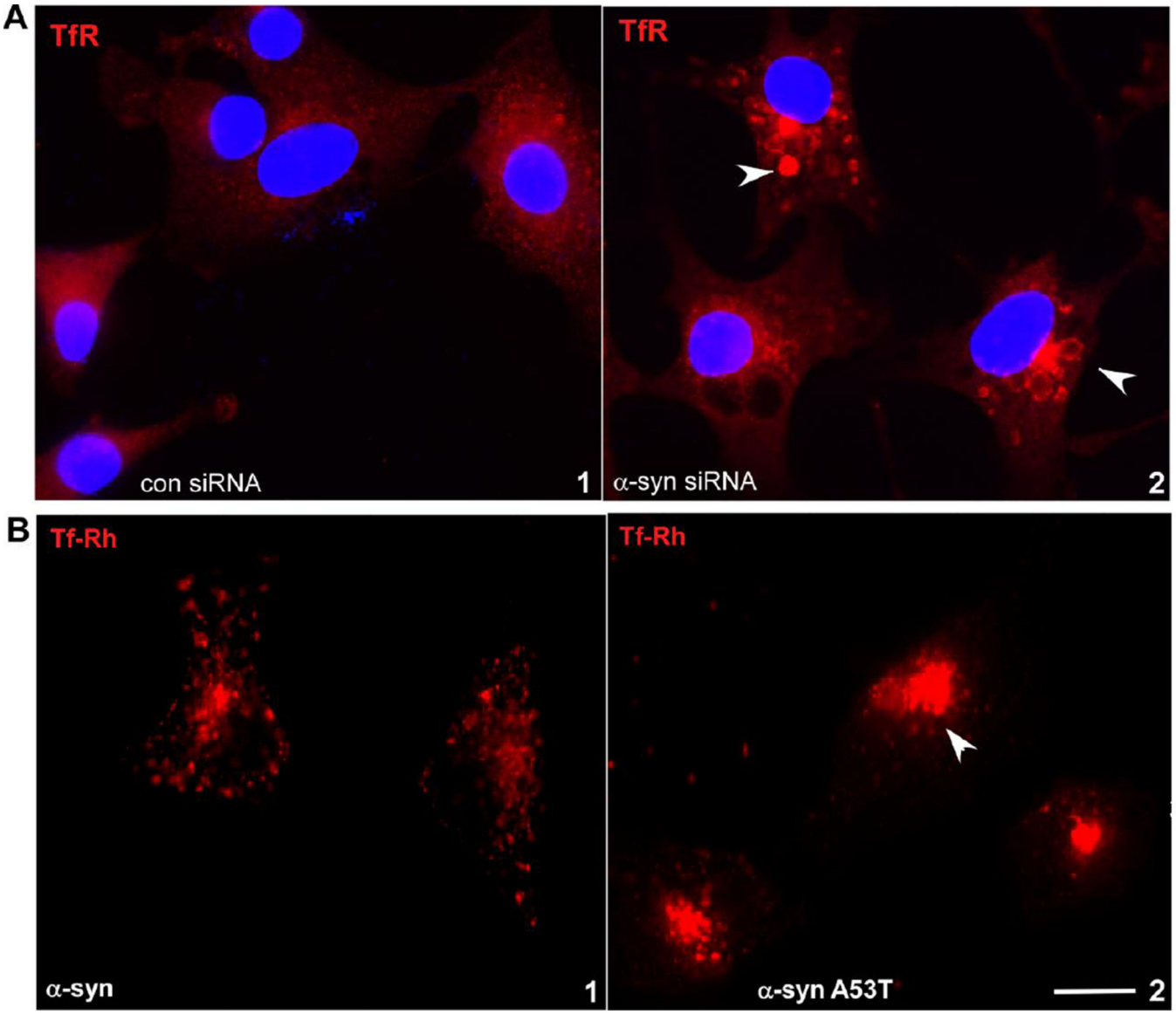

Figure 7. Knockdown of α-syn in RPE cells impairs recycling of TfR to the plasma membrane

(A) Knock-down of α-syn with siRNA results in the accumulation of TfR (red) in perinuclear CREs (panel 2) as opposed to its normal distribution in cells transfected with control siRNA (panel 1). **(B)** Immunoreactivity for TfR (red) is localized to peri-nuclear endosomes in RPE cells expressing mutant α-syn A53T (panel 2) as opposed to its normal distribution in cells expressing α-syn (panel 1). Scale bar 10μm.

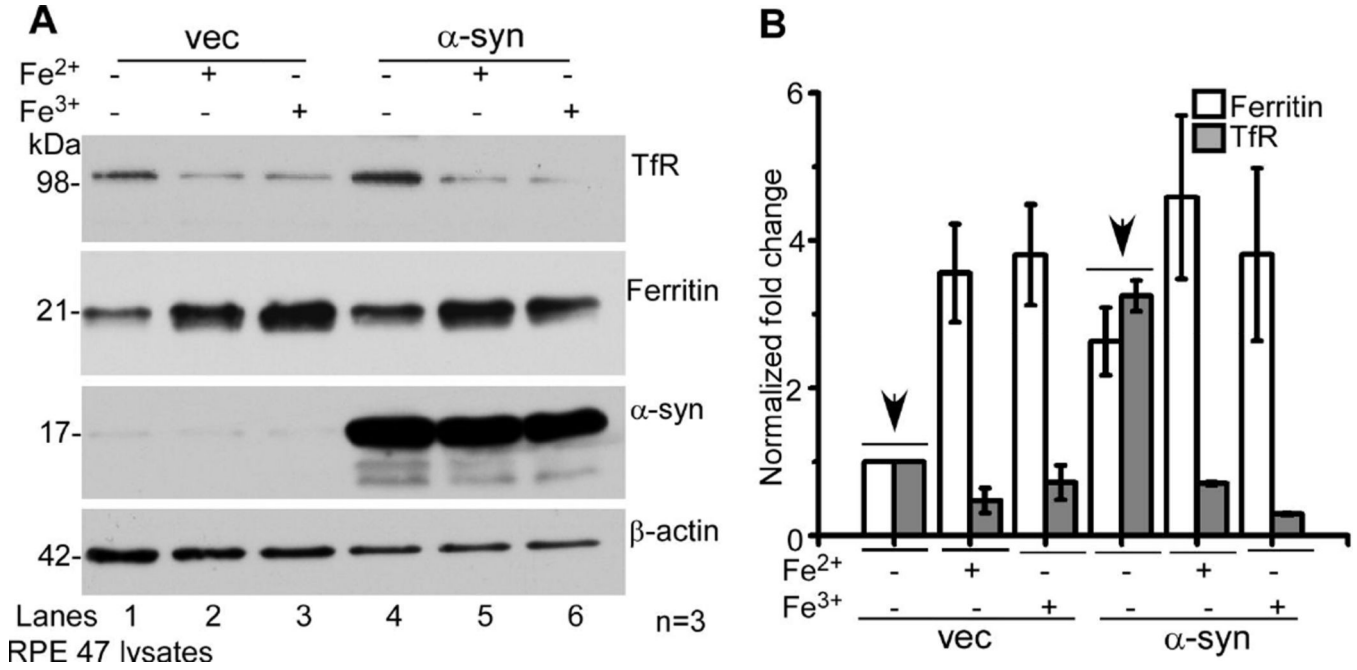

Figure 8. α-Syn does not facilitate the uptake of non-transferrin bound iron

(A & B) RPE cells over-expressing α-syn or vector were exposed to a source of ferric (Fe^{3+}) or ferrous (Fe^{2+}) iron, and lysates were processed by Western blotting. Over-expression of α-syn does not upregulate the expression of ferritin in cells exposed to Fe^{3+} as reported (A, lane 6 vs 3; B) [44]. However, untreated cells over-expressing α-syn show increased expression of ferritin and TfR as noted in Figure 5 C above. Transfected cells show robust reactivity for α-syn as expected (A, lanes 4–6). Reaction for β-actin served as an internal control for protein loading. (n=3). Values are mean ± SEM of the indicated *n*.

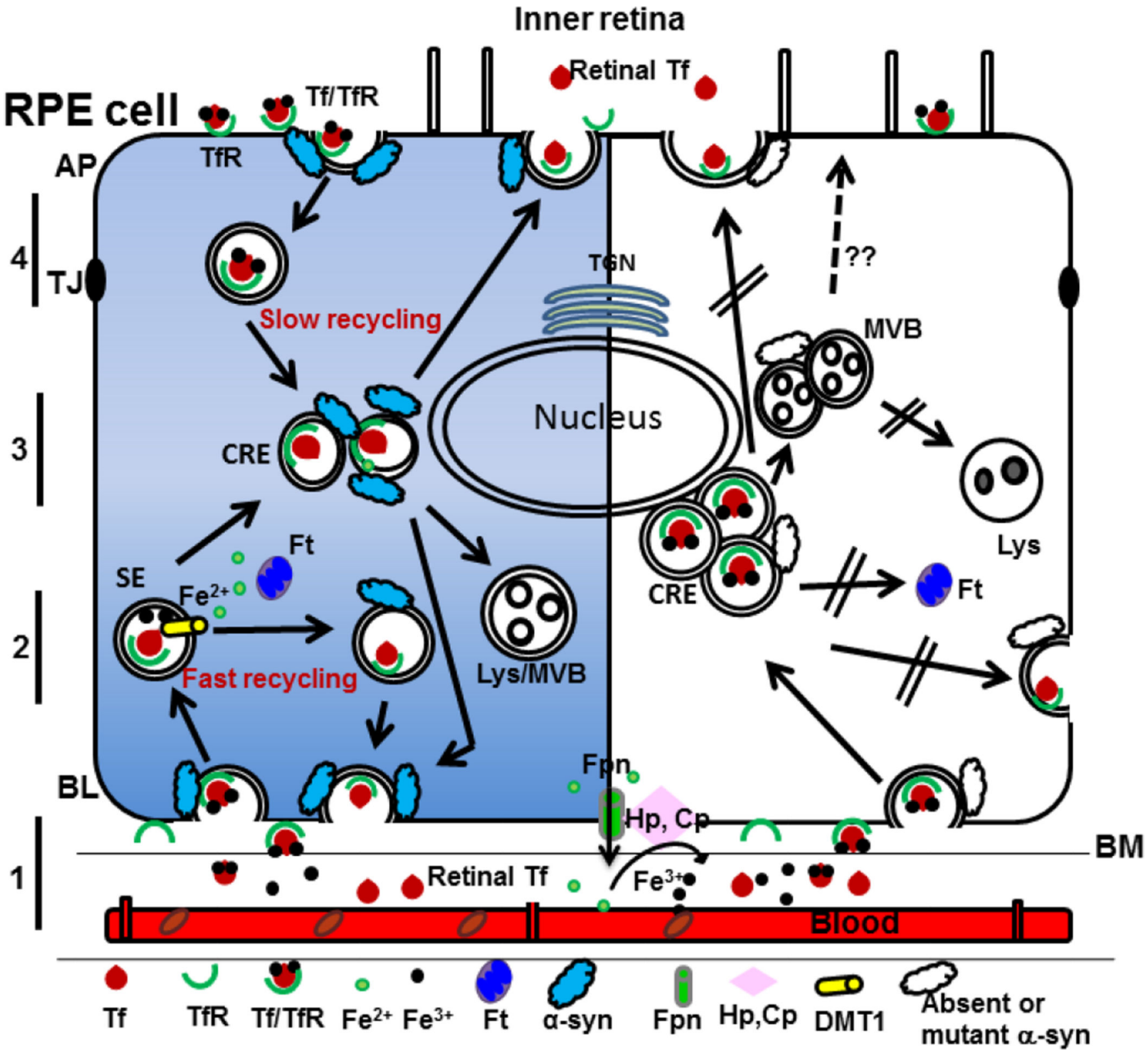

Figure 9. Schematic representation of Tf/TfR trafficking in RPE cells in the presence (left, blue) and absence (right, white) of α-syn

Left panel (blue), based on published results (1) The BL domain of polarized RPE cells abuts the Bruch's membrane that separates the RPE cell monolayer from fenestrated choroidal capillaries. Iron released from plasma Tf is captured by locally synthesized Tf [50] and endocytosed by the Tf/TfR pathway through clathrin-coated pits. **(2)** Tf-bound iron is released in acidic sorting endosomes and transported to cytosolic ferritin across DMT1. Vesicles containing iron depleted Tf/TfR complex are recycled back to the respective plasma membrane domain. This constitutes the fast recycling pathway, and α-syn facilitates different steps of vesicular trafficking by interacting with clathrin, SNARES, and the Rab family of proteins [73, 75, 76]. **(3)** Some vesicles are transported to CREs that are accessible to AP and BL recycling vesicles. Iron depleted Tf/TfR complex is recycled to the AP or BL

plasma membrane domain from this pool by the slow recycling pathway [59, 73, 76]. **(4)** Tf binds ferric iron, and the Tf/TfR complex starts another cycle of endocytosis and recycling [78]). Note: The fast and slow recycling pathways are not restricted to a specific plasma membrane domain; such a depiction in this figure is only for the sake of clarity.

Right panel (white), hypothetical model based on our data. Absence or knock-down of α-syn or the presence of mutant α-syn-A53T impairs several steps in the trafficking of Tf/TfR pathway, resulting in the accumulation of Tf/TfR complex in CREs and/or MVBs. This interferes with the release of iron from Tf and recycling of the Tf/TfR complex back to the plasma membrane. Consequently, levels of total iron, ferritin, and TfR fall significantly, creating a phenotype of iron deficiency.

RPE: retinal pigment epithelium, AP: apical, BL: basolateral, TJ: tight junction, Tf: transferrin, TfR: transferrin receptor, Ft: ferritin, SE: sorting endosome, CRE: common recycling endosome, TGN: trans-Golgi network, Lys: lysosome, MVB: multi-vesicular bodies, Fpn: ferroportin, Hp: hephaestin, Cp: ceruloplasmin, α-syn: alpha-synuclein, BM: Bruch's membrane, DMT1: divalent metal transporter 1.

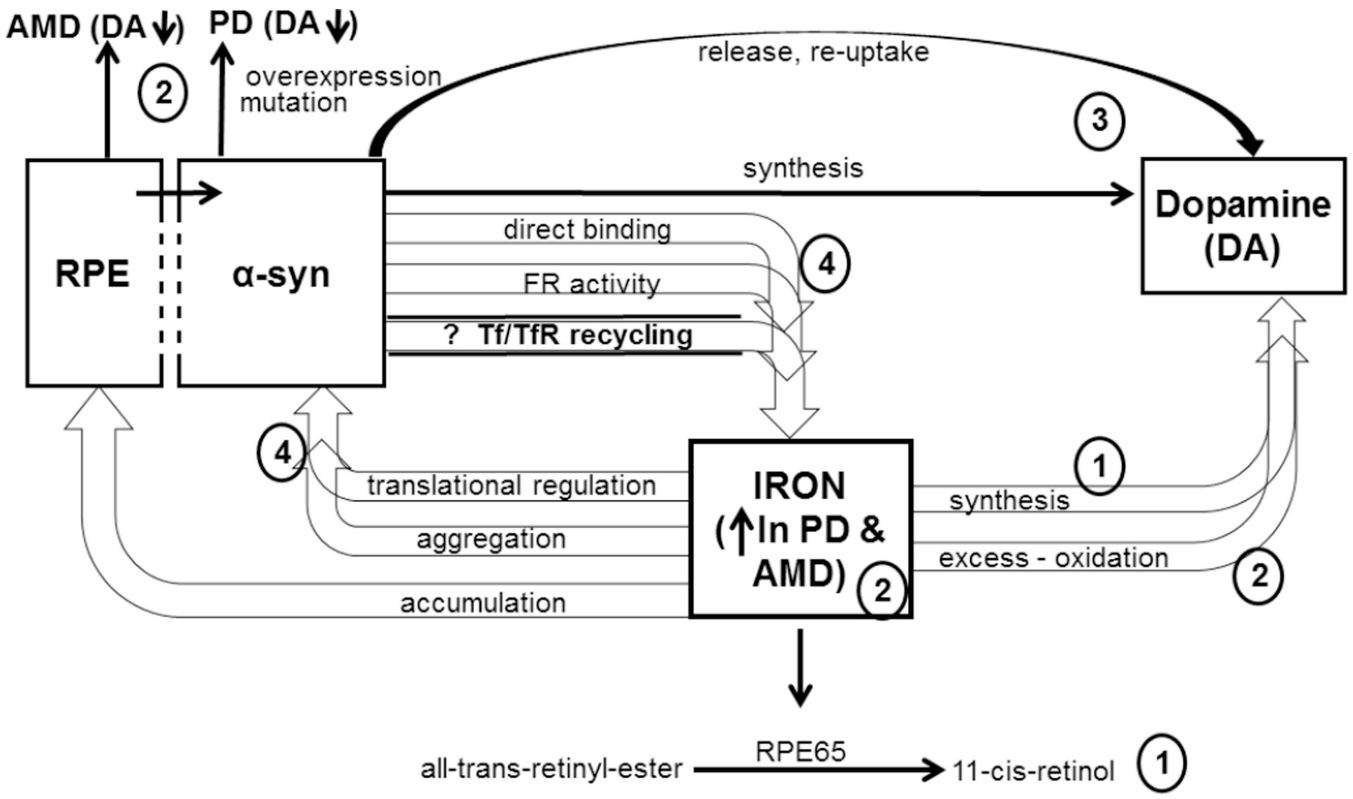

Schematic 1. The central role of iron in retinal physiology and pathology

(1) Iron is necessary for the synthesis of DA and critical components of the visual cycle. **(2)** Excess iron oxidizes DA, a common feature of PD and AMD associated with reduced levels of DA. **(3)** α-Syn mediates the synthesis, release, and re-uptake of DA, and its aggregation due to over-expression or mutation is sufficient to cause PD. **(4)** α-Syn also modulates cellular iron levels, and is itself regulated by iron.